

Experimental Investigation of Temperature and Cork filler on  
The Strength of Tubular Adhesive Joint Under Pure Shear  
Stress



Author

Shamsheer Haider

Regn Number

329952

Supervisor

Dr. Aamir Mubashar

DEPARTMENT OF MECHANICAL ENGINEERING  
SCHOOL OF MECHANICAL & MANUFACTURING ENGINEERING  
NATIONAL UNIVERSITY OF SCIENCES AND TECHNOLOGY  
ISLAMABAD

Experimental Investigation of Temperature and Cork powder  
on The Strength of Tubular Adhesive Joint Under Pure Shear  
Stress

Author

Shamsheer Haider

Regn Number

329952

A thesis submitted in partial fulfillment of the requirements for the degree of  
MS Mechanical Engineering

Thesis Supervisor:

Dr. Aamir Mubashar

Thesis Supervisor's Signature:

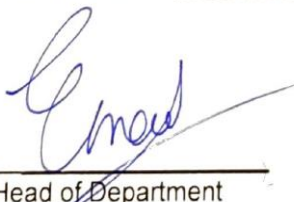
---

DEPARTMENT OF MECHANICAL ENGINEERING  
SCHOOL OF MECHANICAL & MANUFACTURING ENGINEERING  
NATIONAL UNIVERSITY OF SCIENCES AND TECHNOLOGY,  
ISLAMABAD

JULY 2023

**National University of Sciences & Technology****MASTER THESIS WORK**


We hereby recommend that the dissertation prepared under our supervision by: (Student Name & Regn No.) Shamsheer Haider (Reg# 000329952) Titled: Experimental Investigation of Temperature and Cork filler addition on strength of Tubular Adhesive Joint Under Pure Shear be accepted in partial fulfillment of the requirements for the award of **MS Mechanical Engineering degree**.

**Examination Committee Members**1. Name: Dr Emad Ud DinSignature: 2. Name: Dr Zaib AliSignature: 3. Name: Dr Adnan MunirSignature: Supervisor's name: Dr Aamir MubasharSignature: Date: 11/07/23  
Head of Department11/07/23  
Date**COUNTERSIGNED**Date: 11-7-2023  
Dean/Principal

**Proposed Certificate for Plagiarism**

It is certified that MS Thesis Titled Experimental Investigation of Temperature and Cork Filler on The Strength of Tubular Adhesive Joint Under Pure Shear by Shamsheer Haider has been examined by us. We undertake the follows:

- a. Thesis has significant new work/knowledge as compared already published or are under consideration to be published elsewhere. No sentence, equation, diagram, table, paragraph or section has been copied verbatim from previous work unless it is placed under quotation marks and duly referenced.
- b. The work presented is original and own work of the author (i.e. there is no plagiarism). No ideas, processes, results or words of others have been presented as Author own work.
- c. There is no fabrication of data or results which have been compiled/analyzed.
- d. There is no falsification by manipulating research materials, equipment or processes, or changing or omitting data or results such that the research is not accurately represented in the research record.
- e. The thesis has been checked using TURNITIN (copy of originality report attached) and found within limits as per HEC plagiarism Policy and instructions issued from time to time.

  
**Name & Signature of Supervisor** Dr. Amir Mubashar  
Professor  
Department of  
Mechanical Engineering  
(SM:ME) NUST, Islamabad

Signature: DR AMIR MUBASHAR

### THESIS ACCEPTANCE CERTIFICATE

Certified that final copy of MS thesis written by Shamshere Haider Registration No. 000329952 of SMME has been vetted by undersigned, found complete in all aspects as per NUST Statutes/Regulations, is free of plagiarism, errors, and mistakes and is accepted as partial fulfillment for award of MS degree. It is further certified that necessary amendments as pointed out by GEC members of the scholar have also been incorporated in the said thesis.

Signature with stamp:

  
Dr. Aamir Mubashar  
Professor  
Department of  
Mechanical Engineering  
(MOME) NUST, Islamabad

Name of Supervisor: **Dr. Aamir Mubashar**

Date: 11/07/23

Signature of HOD with stamp:



Date: 14/7/23

Countersign by

Signature (Dean/Principle):

Date: 11-7-2023

## **Declaration**

I certify that this research work titled “**Experimental Investigation of Temperature and Cork filler on The Strength of Tubular Adhesive Joint Under Pure Shear Stress**” is my own work. The work has not been presented elsewhere for assessment. The material that has been used from other sources has been properly acknowledged / referred.

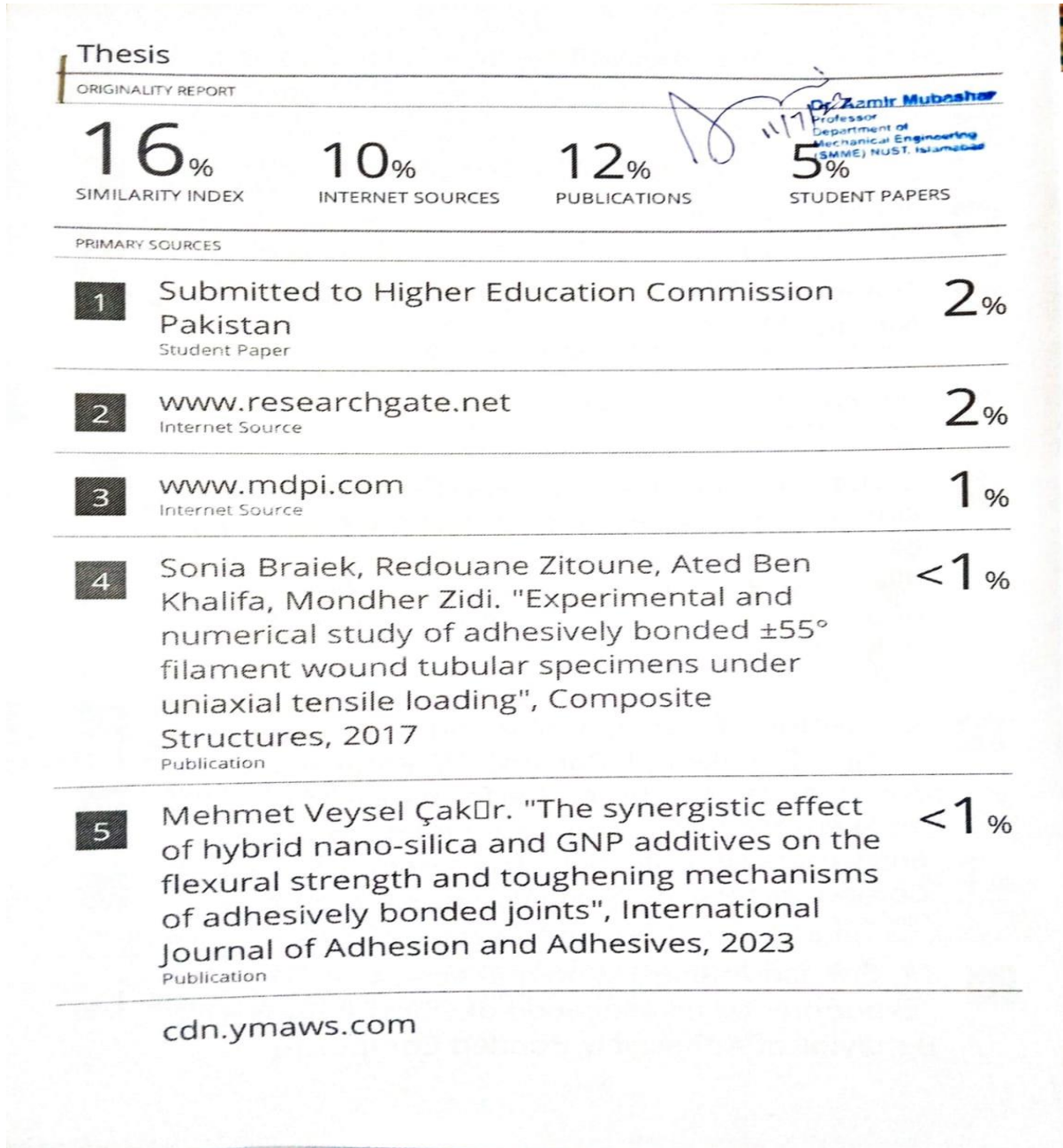
Signature of Student

**Shamsheer Haider**

2020-NUST-MS-Mech-000329952

# Plagiarism Certificate (Turnitin Report)

This thesis has been checked for Plagiarism. Turnitin report endorsed by Supervisor is attached.



## **Copyright Statement**

- Copyright in text of this thesis rests with the student author. Copies (by any process) either in full, or of extracts, may be made only in accordance with instructions given by the author and lodged in the Library of NUST School of Mechanical & Manufacturing Engineering (SMME). Details may be obtained by the Librarian. This page must form part of any such copies made. Further copies (by any process) may not be made without the permission (in writing) of the author.
- The ownership of any intellectual property rights which may be described in this thesis is vested in NUST School of Mechanical & Manufacturing Engineering, subject to any prior agreement to the contrary, and may not be made available for use by third parties without the written permission of the SMME, which will prescribe the terms and conditions of any such agreement.
- Further information on the conditions under which disclosures and exploitation may take place is available from the Library of NUST School of Mechanical & Manufacturing Engineering, Islamabad.



## **Acknowledgements**

I am thankful to God Almighty who have guided me throughout this work and give me strength to overcome all hurdles in every step and for knowledge to complete my thesis. I am pleased to thank my supervisor Dr. Aamir Mubashar for his expert guidance, suggestions, and excellent support during my whole research work. I would like to express my gratitude and heartfelt thanks to my advisor Hassan Ejaz, who supported and guided me throughout the process of research.

*I would like to dedicate this work to my parents and brothers who have always loved and support me. Also, they give me pathway to work hard for achievements in my life.*

## Abstract

The current study presented the combined effects of cork powder and temperature on the strength of tubular adhesive joints under pure mode-II failure. CPVC/Steel and PVC/Steel were two different layouts for joints. Epoxy Araldite-LY-556 and hardener AD-22962 were used as adhesive material, while cork powder was used as filler. Cork powder was added to adhesive material with 0 wt.%, 0.25 wt.%, 0.50 wt.%, 0.75 wt.% and 1 wt.%. Experiment was carried out at four different temperatures of 25°C, 50°C, 75°C and 100°C. Three samples were prepared for each configuration. Adhesive joints were cured at 100°C for two hours. Experiments were carried out on universal testing machine (UTM) under tensile loading. Results shows that for CPVC/steel joint layout overall toughness of joint increases with addition of cork filler, but the failure load decreases with increasing cork filler concentration and temperature. Even though the effects of cork powder remain presented at elevated temperature. Average failure load increased for 0.25 wt.% cork powder at 50°C when compared with failure load of neat adhesive joint for CPVC/steel joint layout. For PVC/steel joint layout it has been observed that highest failure load achieved for neat adhesive at 25-degrees temperature. While the strength of PVC/steel joint decreases with increase in temperature and cork concentration.

**Key Words:** *Adhesive joint, cork powder, tubular adhesive joint, failure load, elevated temperature, strength*

# Table of Contents

|   |             |
|---|-------------|
| <b>Declaration</b> .....  | <b>vi</b>   |
| <b>Plagiarism Certificate (Turnitin Report)</b> .....                       | <b>vii</b>  |
| <b>Copyright Statement</b> .....  | <b>viii</b> |
| <b>Acknowledgements</b> .....   | <b>ix</b>   |
| <b>Abstract</b> .....   | <b>xi</b>   |
| <b>List of Figures</b> .....  | <b>xiv</b>  |
| <b>List of Tables</b> .....   | <b>xv</b>   |
| <b>Chapter 1: Introduction</b> .....  | <b>1</b>    |
| 1.1 Background .....  | 1           |
| 1.2 Research Gap .....  | 2           |
| 1.3 Problem statement .....   | 2           |
| 1.4 Aim and Objectives .....  | 2           |
| 1.5 Research Scope .....  | 3           |
| <b>Chapter 2: Literature Review</b> .....                                   | <b>4</b>    |
| 2.1 Introduction .....  | 4           |
| <b>Chapter 3: Experimentation</b> .....                                     | <b>17</b>   |
| 3.1 Research Methodology .....  | 17          |
| 3.2. Material.....  | 18          |
| 3.2.1 Adherend .....  | 18          |
| 3.2.2 Adhesive.....   | 20          |
| 3.2.3 Filler.....   | 22          |
| 3.4 Procedure for Manufacturing and testing of tubular adhesive joints..... | 25          |
| 3.4.1 Decreasing of steel pipes .....                                       | 25          |
| 3.4.2. Decreasing of Polymers specimens.....                                | 27          |
| 3.4.3. Preparation of neat Tubular Joint.....                               | 27          |
| 3.4.4. Mixing of Epoxy and Hardener.....                                    | 28          |
| 3.4.5. Joining the Steel pipes and PPR socket.....                          | 30          |
| 3.4.6. Curing the joints in oven .....                                      | 31          |
| 3.4.7. Preparation of Tubular joints with filler concentration .....        | 32          |
| 3.4.8. Mixing of epoxy resin, hardener, and cork filler .....               | 32          |
| 3.4.9. Testing of Tubular Adhesive Joint .....                              | 34          |
| 3.4.10. Testing of Tubular Joints at 25 degrees. ....                       | 35          |

|  |           |
|--|-----------|
| 3.4.11. Testing of Tubular Joints at 50 degrees. ....  | 36        |
| 3.4.12. Testing of Tubular Joints at 75 and 100 degrees. ....  | 37        |
| <b>Chapter 4: Results and Discussion.....</b>  | <b>38</b> |
| 4.1. Effect of temperature and cork powder on failure load of tubular adhesive joint for CPVC and Steel: ..... | 38        |
| 4.2 Effect of temperature and cork powder on failure load of tubular adhesive joint for PVC and Steel: .....   | 49        |
| <b>Chapter 5: Conclusion .....</b>   | <b>59</b> |
| <b>References.....</b>   | <b>61</b> |

## List of Figures

|   |    |
|---|----|
| Figure 2.1: Types of tubular adhesive joints [11], [12] .....   | 4  |
| Figure 2.2: Welded joint fatigue life against adhesive bonded joint fatigue life [22] .....                     | 7  |
| Figure 2.3: Average bending strength value of adhesively bonded joint (ABJ) [23].....                           | 8  |
| Figure 3.1: Schematic diagram of cork filler at different amount and at different temperatures .....            | 17 |
| Figure 3.2: Magnetic Stirrer .....  | 23 |
| Figure 3.3: Electronic Balance .....  | 24 |
| Figure 3.4: Cleaning steel surface with acetone .....   | 27 |
| Figure 3.5: Weight measurement for epoxy and hardener .....   | 29 |
| Figure 3.6: Stirring of epoxy adhesive on magnet stirrer. ....  | 30 |
| Figure 3.7 Adhesive joints of steel and PPR pipes at different cork concentrations .....                        | 31 |
| Figure 3.8: Curing of joints in oven at 100 degrees temperature.....  | 32 |
| Figure 3.9: Fixtures for tubular specimens .....  | 35 |
| Figure 3.10: Adhesive joint during testing at 100 degrees temperature.....                                      | 37 |
| Figure 4.1: Force displacement curve at 25°C temperature and at different concentration.....                    | 39 |
| Figure 4.2: Force displacement curve at 50°C temperature and at different concentration.....                    | 40 |
| Figure 4.3: Force displacement curve at 75°C temperature and at different concentration.....                    | 40 |
| Figure 4.4: Force displacement curve of tubular joint at 100°C temperature and at different concentration.....  | 41 |
| Figure 4.5: Average failure load of tubular joint at 25 °C and at different cork concentrations.....            | 43 |
| Figure 4.6: Average failure load of tubular joint at 50°C and at different cork concentrations .....            | 43 |
| Figure 4.7: Average failure load of tubular joint at 75°C and at different cork concentrations .....            | 44 |
| Figure 4.8: Average failure load of tubular joint at 100°C and at different cork concentrations .....           | 44 |
| Figure 4.9: Comparison of average failure load at different temperatures and at different concentrations. ....  | 46 |
| Figure 4.10: Force displacement curve at 25°C temperature and at different concentration.....                   | 51 |
| Figure 4.11: Force displacement curve at 50°C temperature and at different concentration.....                   | 51 |
| Figure 4.12: Force displacement curve at 75°C temperature and at different concentration.....                   | 52 |
| Figure 4.13: Force displacement curve at 100°C temperature and at different concentration .....                 | 52 |
| Figure 4.14: Average failure load of tubular joint at 25°C and at different cork concentrations .....           | 54 |
| Figure 4.15: Average failure load of tubular joint at 50°C and at different cork concentrations .....           | 54 |
| Figure 4.16: Average failure load of tubular joint at 75°C and at different cork concentrations .....           | 55 |
| Figure 4.17: Average failure load of tubular joint at 100°C and at different cork concentrations .....          | 55 |
| Figure 4.18: Comparison of average failure load at different temperatures and at different concentrations. .... | 56 |

## **List of Tables**

|   |    |
|---|----|
| Table 3-1: Properties of Galvanized steel adherend.....   | 18 |
| Table 3-2: Properties of PPR adherend.....  | 19 |
| Table 3-3: Properties of PPR adherend.....  | 20 |
| Table 3-4: Dimensions of CPVC adherend .....  | 20 |
| Table 3-5: The properties of epoxy resin .....  | 21 |
| Table 3-6: Properties of Hardener .....   | 21 |
| Table 3-7: Mix ratio for epoxy and hardener.....  | 22 |
| Table 3-8: Adhesive Joints Properties.....  | 22 |
| Table 3-9: Properties of Filler.....  | 23 |
| Table 3-10: Functional properties of UTM.....   | 24 |
| Table 4-1: Average failure load at different concentrations and at different temperatures .....                                       | 45 |
| Table 4-2: Failure load comparison at different temperatures and at different concentrations with reference to room temperature. .... | 47 |
| Table 4-3: Failure load comparison of neat with different cork concentrations at different temperatures .....                         | 48 |
| Table 4-4: Average failure load at different concentrations and at different temperatures .....                                       | 56 |
| Table 4-5: Failure load comparison at different temperatures and at different concentrations with reference to room temperature. .... | 57 |
| Table 4-6: Failure load comparison of neat with different cork concentrations at different temperatures .....                         | 58 |

# Chapter 1: Introduction

## 1.1 Background

Adhesive joints are increasing due to variety of dissimilar materials joints by replacing formal welded or fastening joints. Adhesive increases the possibility of new joints in structural design, also becoming more cost effective. It also makes possible to join metallic alloys with polymer and composite material without the need to make hole or welding which is the main cause of stress concentration. This led to use of adhesives on large scale in industrial sector replacing conventional methods of joints [1].

The increasing use of adhesive joints in different fields such as civil engineering, automotive and shipbuilding is due to reliability and integrity of bonded joints [2]. There are several benefits associated with the adhesive joints like weight reduction, good mechanical properties, joint of similar and dissimilar material, low stress concentration and corrosion resistance [3]. The coaxial tubular joint has large contact area in limited space for joint. That is why tubular adhesive joints in practical applications is increasing [4].

There are several adhesive joints have been prepared according to their application like single lap joint, single strap, double strap joint, butt adhesive joint, corner joint and most importantly tubular adhesive joint. Tubular adhesive joint show good strength to bending loads because of larger overlap area then other joints. Tubular adhesive joints make the assembly light weight and high stiff [5]. The high mechanical properties and corrosion resistance of fibre reinforced polymer (FRP) has the capacity to replace the conventional metallic piping system [6].

The study shows that tubular adhesive joints depend on different geometrical parameters, adhesive material, overlap length, adhesive impact thickness etc. Experimental analysis shows that with the increase in overlap length, the strength of tubular joint was not linear. Increase in layer thickness, it effects negatively on the strength of the joint. The use of different adhesive gives different level of strength of the joint [7]. Study found that thin adhesive layer, large bond line and higher inner diameter of inner adherend increase the strength of the tubular adhesive joint [8].

In this study mechanical performance of different layouts of tubular adhesive joint under torsional load was analysed. Loctite SI 5699 RTV silicon used as adhesive, stainless steel



and different polymer materials were used as adherend to form a joint. From experimental results it is concluded that surface treatment has greater impact on the strength of joint as results shows that chemical etching surface treatment has higher strength than plasma surface treatment. 90% of von misses' stresses in joint is hold by only 20% of overlap length, so increasing the overlap length after effective length there is no major impact on the strength was seen [9].

The mechanical behaviour and failure mechanism of CFRP and Titanium tubular adhesive lap joint was studied under extreme temperature. The effect of bond line length was also studied to understand the effect on failure load. The results were analysed at cold temperature (CT), room temperature (RT) and elevated temperature (ET). The results shows that mixed failure at ET is due to cohesive failure between first and second ply of the CFRP. It also shows that by increasing the bond-line length on ET conditions the failure load is increased. It is observed that deformation produces stresses which initiate delamination in Ti and subsequently failure of CFRP [10].

Adhesive joint provides high strength to weight ratio with three times more than riveted joint. Adhesive bonding provides sealing and prevent corrosion when joint is with incompatible materials [11].

## **1.2 Research Gap**

- a) Single lap joint has mixed mode failure including mode I and II. So, it is not possible to observe the effect of cork powder addition on each mode of failure.
- b) Tubular joints provide mode-II failure and effect of cork powder addition is unexplored.
- c) The synergic effect of temperature and cork powder addition on tubular joint is also unknown.

## **1.3 Problem statement**

The strength of tubular adhesive joint increase with addition of cork powder at room temperature. Tubular joint operation at high temperature may affect the strength of joint. Synergic effect of temperature and different cork powder addition is unknown.

## **1.4 Aim and Objectives**

The aim of this research is to investigate the strength and failure load of tubular adhesive joint at various cork powder concentration. The objectives of this research are:

- a) To determine the effect of cork powder addition in adhesive under pure mode-II failure.
- b) To investigate the effect of temperature on tubular adhesive joints
- c) To determine the mode of failure in tubular adhesive joints after addition of cork powder and at various temperatures.

### **1.5 Research Scope**

- a) Adherends being used in this research for two different layouts are galvanized steel pipe and polymer (PPR and CPVC) pipe.
- b) Adhesive consists of epoxy Araldite LY-556 and hardener AD-22962 used in this research.
- c) A filler which is cork powder is used with concentration of 0.25wt.%, 0.50wt.%, 0.75wt.%, 1wt.%.
- d) Universal testing machine (UTM) is being used to test tubular adhesive joint.

## Chapter 2: Literature Review

### 2.1 Introduction

The use of adhesive joints is increasing due to their stress distribution and avoid any stress concentration which produce due to welded or bolt joint. The adhesive joint used due to light weight, high strength, resistance to fatigue load and low cost. It is widely being used in aerospace, industry, water supply system and medicine. Tubular joint is used to connect two or more tubular joint. Tubular joint can be of varying diameter. The higher diameter pipe is called chord and smaller pipe is called brace. There are many shapes of tubular adhesive joints such as, K-joint, X-joint, L-joint etc. T-joint shown in Fig. 1(a) that pipes are joined at angle  $90^\circ$  in between them. L-joint shown in Fig. 1(b) are joined together at angle  $90^\circ$  at end of pipe. Fig. 1(c) shows X-joint where four pipes are joined together at an angle of  $90^\circ$  makes the shape like X. Fig. 1(d) shows K-joint in which pipes are joined together at angle less than  $90^\circ$  in centre of main pipe [12].

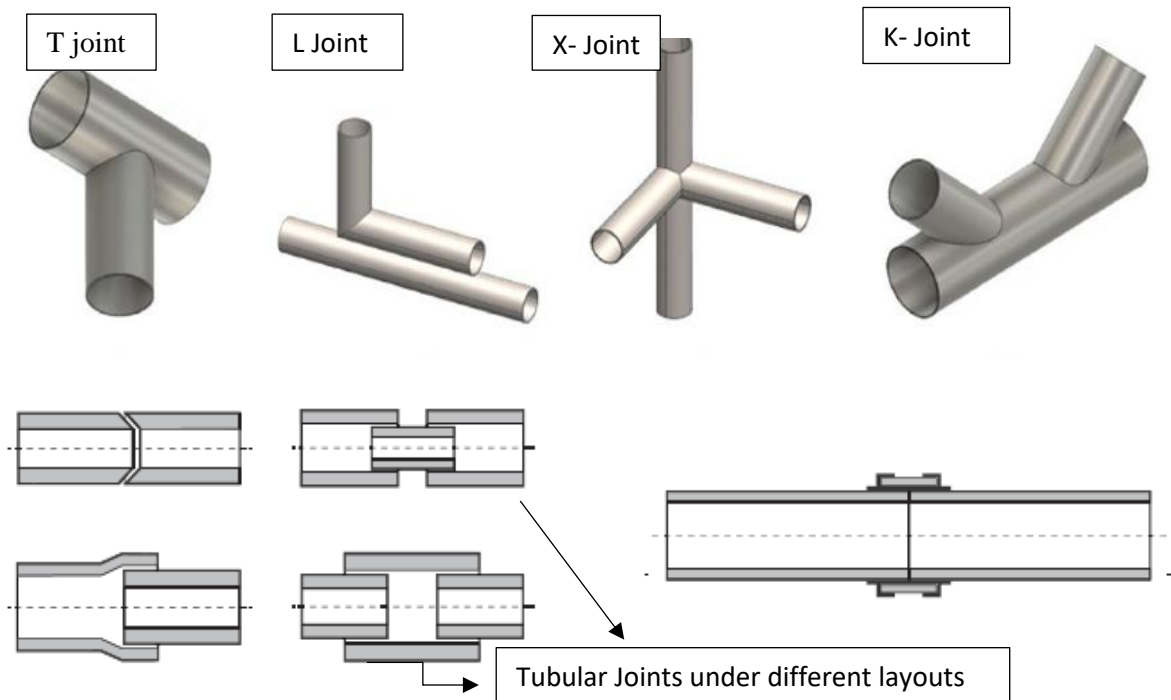


**Figure 2.1:** Types of tubular adhesive joints [12], [13]

Variable stiffness composites (VSC) provide variety in the development of composite material with tailored properties. Using VSC method optimum tubular adhesive joint were developed to sustain tension, shear and thermal loadings. Three axes symmetrical cylinder adherend used. Inner adherend used are linear elastic and outer adherend used is composite

laminate. Joints were developed that can efficiently minimize the stress concentration. Unified theory of tubular adhesive joints was modified to calculate the optimum tub angle variation. Results shows that interfacial shear stress concentration in joints were almost vanished under all loading conditions [14].

In this study the tubular lap joints were chamfered to increase the area of joint that change the scarf angle and that will increase the strength of the joint. Numerical and experimental analysis and cohesive zone model (CZM) were validated. CZM was applied on tubular adhesive joint for angles ( $45^\circ$  to  $3.43^\circ$ ) to analyse the peel and shear stresses. Results shows the improved stress distribution for lower angles for TLJ [15].

The tubular adhesive joints present the better strength in bending due to higher overlap length. Analysis of three different aluminium tubular adhesive joints of different overlap lengths was carried out. Analytical analysis was carried out and compared with numerical analysis using cohesive zone model (CZM). Peel and shear stresses were analysed using (CZM). Using CZM values not identical with the experimental data. CZM failed to reproduce the experimental analysis. CZM is not adequate for highly ductile adhesives [16].

[17] Different T-joints hollow tubular sections made up of glass fibre reinforced polymer (GFRP) incorporated with structural adhesives, carbon fibre and concrete fibre were developed and tested under axial compression. The results of T-joint tubular GFRP with any carbon reinforcement shows brittle failure. The results with carbon concrete filled shows better ultimate strength and ductility. When carbon fibre reinforcement and concrete filled lamination is used it increased the strength by eight-fold and ductility by forty-fold. Design equations and analytical calculations were also developed for future use to develop tubular T-joint.

In this study the effect of temperature on hybrid tubular joint was analysed using Finite Element method to validate the derived analytical equations. Tubular joints consist of carbon fibre reinforced polymer and metallic element. As the material is different for joint, behaviour of temperature will be different on polymer and metallic. To avoid the loss of adhesive material under extreme temperature, glass transition temperature and its effect on the joint was deeply analysed. The results shows that interfacial slip and expansion was anti-symmetry while the strains in joint was symmetric to the centre. It was also seen that increase in temperature has major impacts on the strains developed in the joint. The effect of glass transition temperature on hybrid joint is crucial for integrity of joint [18].

In this article the analysis on the performance of aluminium tubular joint was carried out by varying the overlap length and thickness of tube. Finite element method was used with cohesive zone model (CZM) to analyse the shear strength and joint strength. The results of analysis were validated with previously occurred experimental method. The results shows that shear stresses reduced at centre of overlap length while is maximum at the ends of that. It is also seen that shear stress increases with increase in overlap length. It is also seen that for two different overlap lengths the maximum moment was higher for higher overlapped length [19].

In this article a detailed analysis on the ageing process of tubular adhesive joint was conducted to find the strength of the joint. Three different materials polypropylene, carbon steel and galvanised steel while three different aqueous environment naming supply water, mineral water and demineralised water were applied. Flexible adhesive and stiff adhesive were used. Specimen aged for three months and six months. The results show that longer ageing time has negative effect on the joint. Adhesive joints are better for short interval. It is also seen that joint remained in mineral water environment has high strength as compared to other two aqueous solutions [20].

Influence of the geometrical parameters on the tubular adhesive joint of carbon fibre reinforced polymer with aluminium was studied. Cohesive zone model (CZM) with trapezoidal traction method was used and results were validated with experimental method. Different parameter such as overlap length, bonded area, adhesive thickness, inner and outer tubes taper lengths were considered to find the influence on the strength of the joint. The results shows that pre-treatment of surface has major rule on the strength of the surface. The manufacturing defects such as air bubbles in the adhesive and surface misalignment has no apparent affect on the joint strength. It is found the joint strength increased with increase in overlap length and inner tube diameter with limit on overlap length when effect of overlap length is not increased [21].

This study analyses the damage and strength of carbon fibre reinforced polymer and titanium tubular lap joint using hybrid adhesive design. Damage model performed using finite element analysis using cohesive zone model (CZM) to understand the damage and stress analysis. Numerical damage model validated with published experimental data. Brittle and ductile adhesive used in this study to see the effect of hybrid adhesive. Four different configuration was analysed which contain brittle adhesive, ductile adhesive, brittle ductile brittle (BDB) and ductile brittle ductile (DBD). Results shows that brittle material has low

strength and less displacement when compare with ductile material. While DBD has high strength and displacement as compared to BDB [22].

This study based on fatigue life prediction based on Arcane test results of real structural joint of complex geometry. Stress life approach used to get the master stress life curve. The master class curve used to predict the fatigue life of the joint and then it is compared with the welded joint. The results shows that adhesive bonded joint has higher life cycles against higher load when compared with welded joint [23].

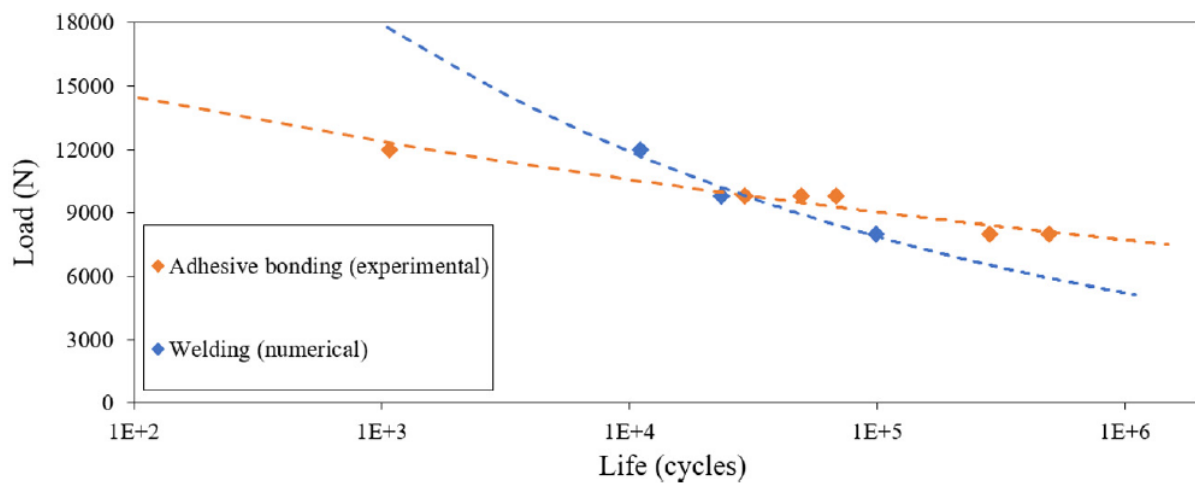


**Figure 2.2:** Welded joint fatigue life against adhesive bonded joint fatigue life [23]

In this research the synergic effect of hybrid nano-silica and GNP additives was studied on adhesively bonded single lap joint. Total additive ratios of 0.5%, 1%, 1.5%, 2% and 2.5% by weight was prepared and tested under three-point bending. The ratios of nano-silica to GNP of 1:2, 1:1, 2:1, 3:1 and 3:2. The results shows that best performance was obtain at 1.5% nano-silica +0.5% GNP sample at particle ratio of 3:1. The flexural strength was increased by 51.3% when compared to neat adhesive of araldite 2014. It is also seen that joint improved the interfacial interaction of nanoparticles. The joint increased the resistance of crack deviation and crack bridging [24].

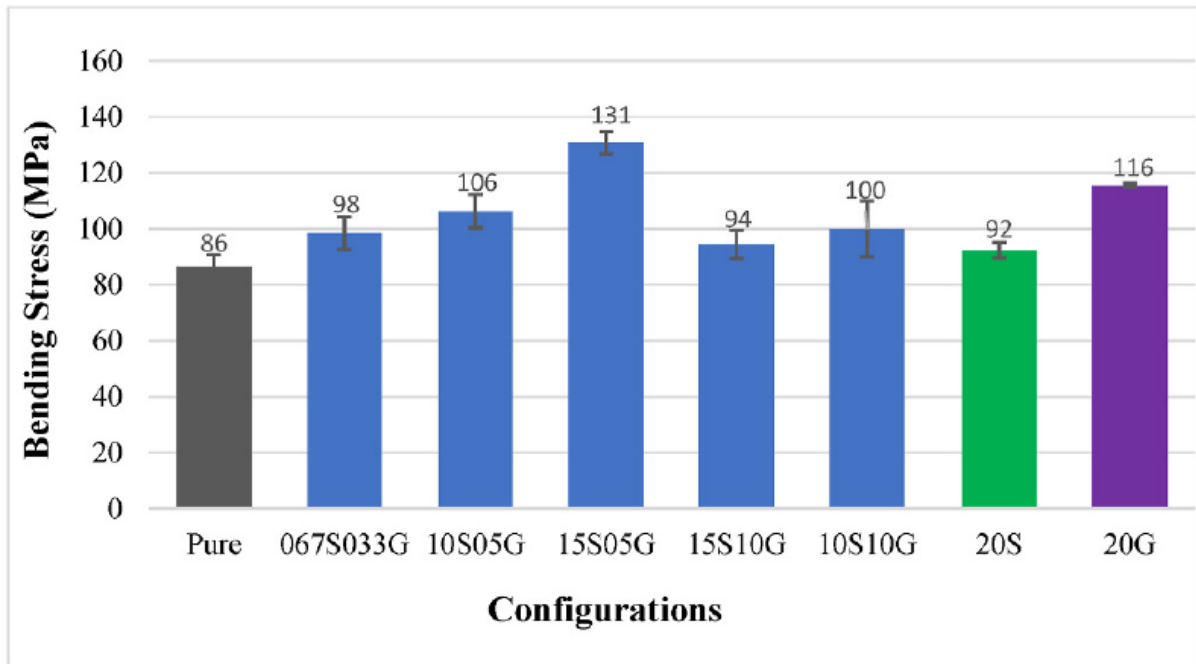


**Figure 2.3:** Average bending strength value of adhesively bonded joint (ABJ) [24]

In this study industrial case study was carried out in which welded joint is compared with the adhesive joint. The boom structure of hydraulic machine was used in this research. Three different overlap length full, 50% and 30% of structure was used to see the strength and compared with welded joints. Methacrylate adhesive was used in this experimental research. Results shows that adhesive joint can replace the welded joint and 30% overlap length structure has higher failure strength then the welded joint [25].

This article present study on adhesive joint, self-piercing joint (SPR) and hybrid joint on H shaped aluminium under tension. Joint strength, stiffness and energy absorption were compared for aluminium sheet metal alloy and three different sheet thickness. The results shows that adhesive joint show 20.5% more strength, 422% higher stiffness than SPR joint. SPR joint shows higher energy absorption up to 352%. It also been seen that hybrid joint with sheet thickness of 3mm shows reduced strength and stiffness then the adhesive joint. This study also helps to identify sheet thickness, type of joint used in future application. This study also helps to improve the hybrid joints in future [26].

Adhesive bonding of tubular structural steel studied in that article with the purpose to apply traditional joining technique on large scale. Polyurethan and epoxy as adhesive material were selected and tested under required strength with lap shear strength should be greater than 10 MPa and glass transition temperature should be greater the 80 °C. Different parameters were

studied such as adhesive type, overlap length, adhesive layer thickness and manufacturing imperfections. Adhesive joints were tested under quasi-static loading with diameters from 42mm to 300mm. The results show that both (Polyurethan and epoxy) adhesives exhibited linear behaviour and brittle failure. When adhesive joints cured at room temperature, the polyurethan shows twice the resistance in tension when compared with the epoxy. Mechanical performance of polyurethan is more than epoxy. It is also found that with increase in overlap length the strength of the joint increases but increase in bond thickness has negative impact on joint strength [13].

The paper analyses the aluminium tubular adhesive joint by outer chamfering technique to improve the static strength. Numerical analysis was verified using experimental method. The numerical method was based on finite element analysis and cohesive zone model to predict the maximum load ( $P_m$ ). The test results shows that short bond length show high strength with brittle adhesive. While with higher bond length show better  $P_m$  with less strength. Chamfered exhibit the gradual decreasing peel stress and shear stress [27].

This paper [28] presented the detailed numerical and experimental study of tubular adhesive joint to analyse the strength of the joint and propagation to failure. E glass reinforced polymer composite tubes were manufactured using three different types of thermoset resins which include E glass vinylester/411, E glass/vinylester 470 and E glass/isophthalic polyester. The study shows that E glass/vinylester 411 exhibit best tensile properties as compared to other materials. This due to compatibility of resin with the adhesive. During experimental study it was noticed that E glass/vinylester 411 shows two behaviours, one was linear elastic behaviour and second was nonlinear behaviour for crack initiation and crack propagation. X-ray technique on specimen show several damage mechanisms. Decohesion of adhesive layer, delamination between adhesive layer and inner layer. Matrix cracking of inner tube. The numerical study based on Meso-model concept shows excellent agreement with the experimental method with small difference of 4.5mm displacement.

Tubular butt joint was used to measure the properties of epoxy film adhesive in torsion and tension. To determine the stress-strain curve of adhesive local strain or deformation needs to be determines. For that purpose, two different strain measurement techniques were used. One was digital image correlation (DIC) system and second one was pacitive sensor combined used in this experimental study. This system allows decoupled measure of axial and torsional movements. The result shows suitability for both systems [29].



This study [30] was carried out on computational fluid dynamics and fluid structure interaction which is based on modelling and simulation analysis to investigate the adhesion failure in tubular adhesive joint. For that purpose, steel pipes with sockets were selected with geometrical parameters like gap between the adherends, overlap length and adhesive thickness have been optimised to minimize stress concentration in pipes joint for turbulent flow liquid. The results carried out through ANSYS analysis compared with the experimental results. The results were taken failure index against the overlap length. It was seen that failure index value was minimum for overlap length with value of 32mm. So, it was considered that 32mm overlap length is optimized length for the current study.

The study was carried out to analyse the cyclic performance of bonded sleeve beam-column connections FRP tubular section. Tubular specimens with end plates and bolted joints were tested under cyclic loads. Different responses were gained through experimental testing such as moment-rotation response behaviour characterized by rotational-stiffness, ultimate moment, and rotational capacity of specimen. Performance was based on ductility and energy dissipation capacity. GFRP square hollow section used in that analysis. Results from the experimental analysis exhibit that bonded sleeve failure start with the yielding of steel endplate. After yielding failure, cohesive failure was seen at the interface between steel tube and GFRP column. It was also found that material with same thickness of endplates shows similar moment rotation responses. Results of proposed modelling approaches shows accurate moment-rotation responses [31].

This article investigated the fatigue life analysis of uniaxial and multiaxial life of adhesively bonded butt joint using stress-based failure models. The analysis was made to analyse the equivalent stress amplitude, loading frequency and equivalent mean stress on the fatigue life the specimen. The experimental results exhibited that uniaxial tensile cycle is shorter than uniaxial torsion cycle. Effects of non-proportional loading path on cyclic loading is greater than the proportional loading path. Equivalent stress amplitude, equivalent mean stress and loading frequency has effect on the fatigue life the adhesive butt joint [32].

This paper analytically analysed the tubular single lap joint of functionally graded modulus adhesive (FGA). The adhesive bonding of dissimilar material suffers stress concentration at the bond-line which cause failure of the joint. It is proposed in literature that FGA with nanoparticles distribute inside the polymer to overcome the problem of stress concentration at bond-line. The theoretical capability of FGA must change the elastic properties

of as function of reinforcement inside the bond-line. This capability can be exploited to reduce the stress concentration produce inside the joint. It is also possible to change the shear modulus of the joint. It is possible that adhesive maximize the load carrying capacity [33].

In this article auther analyse the static and dynamic strength of epoxy adhesive in high thickness joints. It is expected that with the increase in joint thickness its properties may change. In static and dynamic experimental analysis both the interfacial and intrinsic properties of the adhesive need to be verified. In this analysis different geometries were analysed such as dog bone shape, hollow cylindrical and bonded joint, specially designed hollow cylindrical joint and butt joint. Experimental analysis was carried out under quasi-static and fatigue loads at variant conditions. Due to complex geometry and difficulty on analysing the data, the results were based on probabilistic approach rather than realistic approach. So, it is required to extend the data to establish realistic approach [34].

This article [35] predicts the failure load of tubular bonded structure using coupled criteria. Both analytical and experimental analyses were done and compared. In this study adhesive was epoxy based bi component resin. Arcan test was used to determine the mechanical properties of the adhesive material. Substrate material was 2024 aluminium-based alloy. Coupled criteria based on two different conditions. One was stress criteria to describe the micro crack and other one was energetic criteria related to nucleation of micro crack to macro crack. The Arcan experimental results shows that material behaviour was brittle, the failure surface shows the mixed failure (cohesive and adhesive). Behaviour of adhesive material shows that failure load increases with the loading rate. Normal displacement decreases with the loading rate. It was also found that failure load increases with the bond length. The tests were performed to analyse the effect of adhesive thickness on the failure load, it was found that with the increase in thickness the failure load decreases.

Failure analysis of composite bonded joint with internal pressure and axial loading was carried out in this article. The internal pressure is experienced by the pipes used for flow of different fluids. The finite element analysis based on modelling and simulation was carried out to analyse the failure of the joint. The joint consists of two inner adherend and one outer adherend socket. These are joint by FRP. The results shows that peel stresses variations were seen in mid plane of all socket joints. Peel stresses were observed near the free edges and adherend junction. Peel stresses remains constant over the overlap length. From the analysis it has been concluded that inner adherend-adhesive is more prone to adhesion failure [36].

The author analysed the adhesive solutions in multi material cylinder joints with elastic solution. The analyses carried out using analytical and finite element method to get the results and compared both. The assembly is based on titanium cylinder and tube adherends with homogenous adhesives under tensile load. In this analysis shear and peel stresses were analysed and their region of presence. Results shows that shear and radial stress distributions are highly dependent on axial stiffness mismatch. Shear stress near the ends of the adhesive layer remains present due to singularity. Shear stress along the radial direction present uniform [37].

In [38] author investigated the CFRP (Carbon fibre reinforced polymer) strengthened circular hollow section (CHS) beam using experimental and numerical method. Different orientations of beam layers were used in this study. Mid span deflection, failure load and service load were recorded. Numerical analysis was also carried out to analyse the validity of the study. The results shows that three different layers were used to increases the ultimate strength of the joint. More than 33% increase in ultimate strength of the joint was seen for strengthened beam compared to unstrengthen beam. More than 50% increase in service load was seen for different layouts. Mid span deflection for strengthen beam was seen more than unstrengthen beam. The higher stiffness was seen for strengthen beam when load increased 40KN. Finite element analysis was carried out using ABAQUS software. Results for mid span deflection, failure load and service load were analysed and compared with the experimental results. The results of numerical analysis show good agreement with the experimental results.

The study [39] carried out on web/flange reinforcement glass fibre reinforcement polymer (GFRP) bonded beams influence on mechanical response using epoxy. Two different 2D and 3D models were developed. 2-D model help to understand the bonding joint and understand the influence of different reinforcements on the distribution of stress in adhesive joint. 3-D model was developed to understand the influence of reinforcement on the mechanical behaviour which help to predict failure and stiffness. The model results show 20% increase in failure load and 12% increase in the flexural stiffness when compared with the existed pultruded models.

The current article presented the durability of glass fibre reinforcement polymer (GFRP) for circular hollow section (CHS) under accelerated sea water [40]. The CHS was studied with and without GFRP at ambient and 50°C temperature. Beams were tested under four-point bending. Results shows that various failure modes were observed. The major failure mode was observed near the loading point due to accelerated corrosion effect. The embedded

GFRP achieved high ultimate strength under saline water conditions. The beams show similar behaviour under low loads. It was also seen that there is no significance of ambient and elevated temperature. To introduce the effect of elevated temperature, it is required to decrease the density by keeping % mass loss. The comparison of experimental and theoretical model was in good agreement with each other.

The author presented the performance and fatigue analysis which was carried out on Pultruded GFRP assembled space bridge in reference to pedestrian bridge. The structure is based on GFRP circular hollow section with novel steel connection. Peak picking was used to collect the data of free vibration test. Stochastic subspace identification system used to analyse the natural frequencies, damping ratios, and mode shapes. Space frames consist of a span of 8 m, width 1.6m and height 1.13m. Results of natural frequencies was collected for first five order mode, third mode of value 21 Hz shows bending mode, the other four, modes were torsion modes. FE modelling results shows good similarity with the bending modes achieved through experimental process [41].

The Performance analysis of joints based on cork and ceramic matrix composites for thermal protection of structure was described in this study. Joints made up of NORCOAT LIEGE cork and ceramic matrix composites were prepared. Shear stress under ambient conditions and under liquid nitrogen conditions were studied. The ultimate shear strength under normal conditions varies between 0.52 and 0.78 MPa. Under the liquid nitrogen temperature, the shear strength increases by 80% but the shear strain decreases up to 55%. According to application it is required shear strength up to 0.1 MPa and temperature range of (700-900) °C [42].

Current study is carried out to analyse the responses of metallic fibre reinforced adhesive epoxy under mixed mode fracture. The object of this study is to see the effect of metal fibre reinforcement effect on aluminium epoxy joint under mixed mode loadings. Experimental analyses were carried on double cantilever beam (DBC), single led bending (SLB) and end notched flexure (ENF). Loading was applied under pure mode I, pure mode II, and mixed mode. Distance between the metal fibre was taken as key parameter in the analysis. Experimental result shows that the highest fracture energy was obtain under mode I load conditions for reinforced adhesive joint about 12 times more than non-reinforced adhesive. It was also found that joints with lower distances for metallic reinforced has higher fracture energy. Mixture of failure loads were seen during the analysis with microscopic photography

were seen such as fibre pull out, fibre bridging, fibre slippage and shear banding in rough fracture surfaces [43].

In this article the author presented the effect of cork particles reinforced with adhesive on toughness and effects of size of particles, amount, and effect of surface treatments. As it is known that addition of nanoparticles or microparticles enhanced the strength of the joint by absorbing more fracture energy. Natural micro particles of cork are used in adhesive to increase the toughness of brittle epoxy adhesive. Size of particles used were between 38-53 and 125-250  $\mu\text{m}$  were added in adhesive araldite 2020. Volume of cork added 0.25% and 1%. Results were analysed using fracture analysis by three-point bending. Also, to analyse the experiments Taguchi design was used. Results shows that plasma treatment become the cause of erosion in cell wall, and it reduces the thickness of the walls. It was also found that size of particles, amount and surface treatment has impact on the toughness of the adhesive joint. Highest influence on toughness of joint was seen for surface treatment, then particles amount, and less effect was seen for particle size [44].

The author presented the numerical prediction of adhesive joint which has been already prepared for experimental analysis and results were compared with each other. Experimental analysis was based on two different adhesives, three overlap lengths and different thicknesses were used for adhesive steel connection. So, the results were used for the formulation of suitable failure criteria of the adhesive joint. Numerical model was developed for the results obtained in experimental method. The bonded joints taken simultaneously under the shear and transverse tensile strengths altogether. Results shows that direct stress capacity is not able to correlate with the observations. With the increase in overlap length, joint strength increased, but also peak stress increases. It was also seen that with the increase in thickness of the joint, the strength of the joint decreases. Probabilistic method was also developed with measure the average failure loads and characteristic values as well [45].

The extended finite element method to analyse the model of tubular adhesive bonded joint was presented in this study. Analysis was carried out with different bond lengths and different adhesives. The numerical study made possible to analyse the peel and shear stresses. The results shows that shear stresses are more significant in bond strength as compared to normal peel stresses in the joint. Peel stresses increases with bond length but reduce the bond efficiency for brittle efficiency. Shear stress also increase with overlap length but for higher overlap lengths. Study shows that brittle adhesive highly effected by peel and shear stress [46].

The present study discusses the joint of moulded wooden with steel in form of tubular. The numerical and experimental study was carried out in analysis of thin-walled wood and tubular steel joint. Tensile and compressive stress were applied on the joint to determine the load carrying capacity of joint in experimental analysis. While the probabilistic approach was used to analyse the numerical model which taken to determine the properties of the brittle adhesive and to determine characteristic strength of the joint. Results shows that wooden sample failed inside the steel tube. In tension and compression tests it was observed that crack initiation starts from the transition area and then propagated throughout the joint length. Both experimental and numerical analysis shows that with increase in overlap length, ultimate load converges [47].

The present study analyses the strength and performance of single lap joint for dissimilar material using aluminium (Al) and glass fibre reinforced polymer (GFRP) as adherends and ZnO was used in adhesive to make the joint. Non-destructive method such as ultrasonic testing and x-ray testing radiography was used to analyse the joints. The results show surface treated specimen present the highest load carrying capacity with increase in 154.67% and bond strength with increase in 154.67% when compared with non-treated surface of adherend. 182.1% increase in strength of adhesive was seen when ZnO was added [48].

The author presented the effect of Boron nanoparticles reinforced in nanocomposites and bonded joints on the mechanical performance under sulphuric acid environment. The samples consist of composites and SLJ were placed in acidic environment at 40°C and for 20, 40 and 60 days to evaluate the effect of sulphuric acid on the material. Two different analysis consists of Fourier transform infrared spectroscopy (FTIS) and scanning electron microscopy (SEM) were performed to analyse the damage of surfaces due to acidic environment. Results shows that composites and SLJ present higher performance reinforced with boron nanoparticles as compared to unreinforced specimens [49].

The current study presented the effect of hexagonal boron Nitride (h-BN) and hexagonal boron carbide nanoparticles on epoxy composite adhesive and single lap joint (SLJ) in ageing and degradation of mechanical and thermal properties. Doped and undoped joints were exposed to water for 20, 40 and 60 days. There were several tests such as FT-IR, SEM, DSC, DMA and tensile tests were performed to find the effects of nanoparticles on joint. It was found that doped adhesive with h-BN and h-BC shows slower ageing and degradation of joints as compared to undoped adhesive joint. Degradation rates in undoped adhesive joints were

found 30% and 29% while the degradation of joints doped joints show 16% and 18% rates. While the mechanical properties of undoped, h-BN and h-BC joints were recorded 34%, 19% and 20% [50].

In current study author presented the theoretical analysis of tubular bonded adhesive joints which is functionally graded bond line under axial loading. The tubular adherends are based on similar and dissimilar tubes with functionally modulus graded bond line length (FMGB) adhesives. Axis symmetric elastic analysis was carried out to analyse the peel and share stresses in the bond line. The results were compared with mono-modulus bond line (MMB). Results shows that with the increase in bond line the peel and shear stresses distribution along the bon line was more uniform when compared with the BBM. Stress distribution in FMGB was very less as compared to MMB as shear stress distribution losses its symmetry and peel stress losses its anti-symmetry. Results also show that with the increase in adhesive thickness the peel and shear stress distribution become more uniform when FMGB compared with MMB [51].

The author presented the nonlinear analysis of tubular single lap adhesive joint in torsion. Composite adherends were selected to make tubular joint to analyse the stress and strain in torsion. For that analysis nonlinear approach was used, first stress and strains were calculated under general loading and then iterative method was used for calculations. Results from numerical analysis shows that stress concentration produced in nonlinear approach is much relieved as compared to linear analysis. That shows that strength of the joint is underestimated in case of linear analysis [52].

## Chapter 3: Experimentation

### 3.1 Research Methodology

Many experiments on tubular adhesive joints have been done and different are being done, to find the strength of the joint. Different material, adhesives or cork material are tested but there is need to check the strength of the tubular joint using different material, adhesive, cork material at different temperature. In this experiment temperature range of 25–100-degree temperature has been used under different concentration of cork material. Specimen used in this experiment consist of dissimilar adherends (galvanized steel and polymer) to evaluate the strength of the joint under pure share. Two different layouts are being used, one is galvanized steel and Polypropylene random (PPR), the other one is galvanized steel and chlorinated poly vinyl chloride (CPVC). In both layouts galvanized steel remains as inner adherend. Universal testing machine is being used to perform the experiments under tensile testing. Design of the experiment for the present work is shown below.

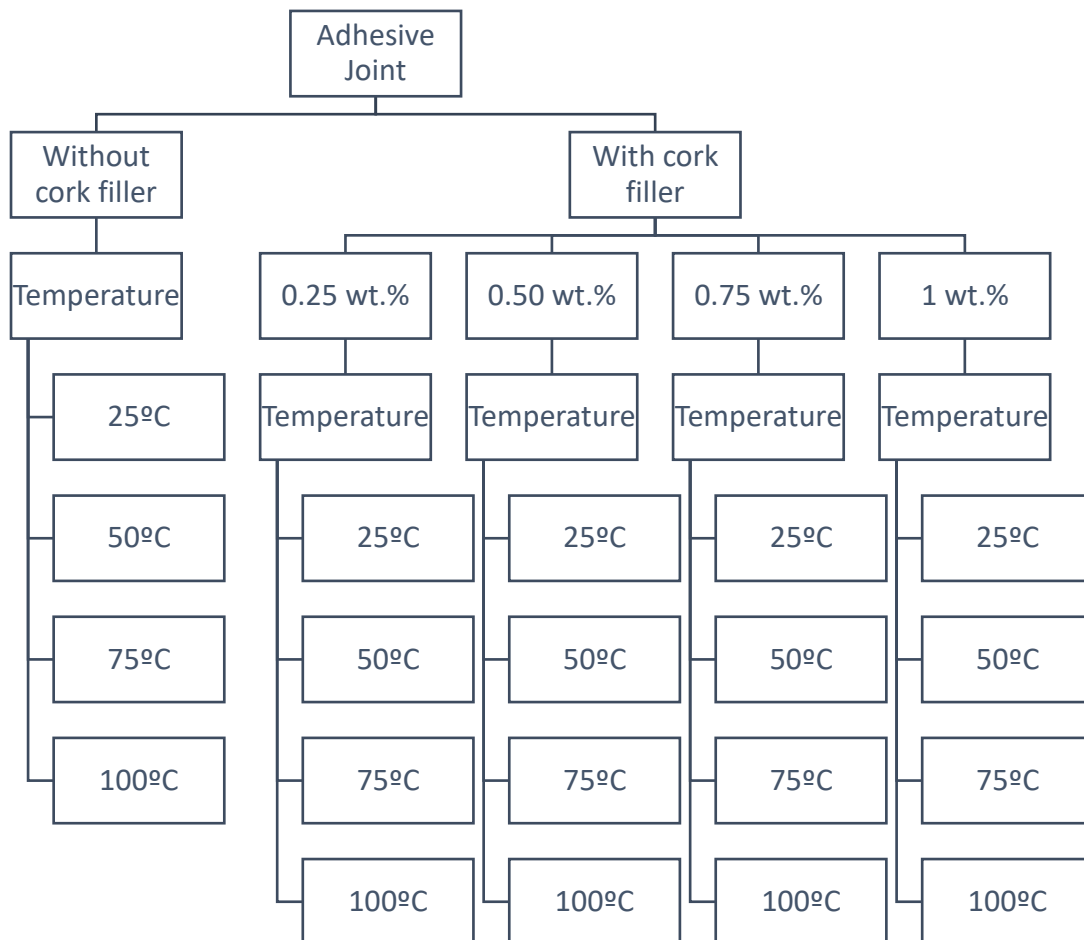


**Figure 3.1:** Schematic diagram of cork filler at different amount and at different temperatures



## 3.2. Material

### 3.2.1 Adherend

Adherend used in that research are Galvanized steel pipe, PPR pipe and CPVC pipe to make two different layouts in which steel pipe remains as inner adherend material.

#### (a). **BS1387 Galvanized Steel Pipe**

##### (i). **Characteristics of Galvanized Steel Pipe**

Galvanized steel is coated with zinc material which save steel from direct contact with the atmosphere and save it from corrosion. In this process the surface of steel becomes more durable. Galvanized steel is widely used in marine application, hot and cold-water transportation. In petroleum industry it is used to transport low pressure oil and oil well pipes. These pipes are also used in trestle bridges.

##### (ii). **Number of Galvanized steel pipe samples**

Each part of galvanized steel is 2.5in lengthy. One sample required two steel parts. Total number of steel samples required to make two different layouts were 240. Each layout required 120 samples, along each parameter 3 samples and total number of tests were 20.

##### (iii). **Properties**

**Table 3-1:** Properties of BS1387 Galvanized steel adherend

|          |                   |                        |
|----------|-------------------|------------------------|
| <b>1</b> | Young's modulus   | 210 GPa                |
| <b>2</b> | Yield's strength  | 300 MPa                |
| <b>3</b> | Ultimate strength | 400 MPa                |
| <b>4</b> | Density           | 7850 kg/m <sup>3</sup> |
| <b>5</b> | Poisson's ratio   | 0.3                    |

##### (iv). **Dimensions**

Outer diameter of Galvanized steel sample =  $26.67 \pm 0.2$ mm

Inner diameter of Galvanized steel sample =  $22 \pm 0.1$ mm

Length of the Galvanized steel sample =  $63.5 \pm 0.2$

**(b). Polypropylene Random (PPR) Adherend**

**(i). PPR characteristics**

PPR pipe is rigid and cylindrical made through continuous extrusion process. These pipes are heat resistant, corrosion resistant, its ability to carry fluids up to 100 degrees. It is widely used in cold and hot water distribution, wall cooling and heating system, under floor heating system and radiator connections.

**(ii). Number of PPR samples**

Total number of PPR samples used are 60. As 3 PPR samples used for every parameter.

**(iii). PPR Properties**

**Table 3-2: Properties of PPR adherend**

|          |                      |                       |
|----------|----------------------|-----------------------|
| <b>1</b> | Tensile modulus      | 900 MPa               |
| <b>2</b> | Thermal conductivity | 0.24 W/(mK)           |
| <b>3</b> | Density              | 905 kg/m <sup>3</sup> |
| <b>4</b> | Melting temperature  | 210-220 °C            |

**(iv). Dimensions**

PPR sample length = 38mm

PPR outer diameter = 36.5mm

PPR inner diameter = 26.7

**(c). Chlorinated Poly Vinyl Chloride (CPVC) Adherend**

**(i). CPVC Characteristics**

CPVC is widely used in industrial application where high temperature, high pressure and resistant to corrosion is required. CPVC has high glass transition temperature and outstanding mechanical properties.

**(ii). Number of CPVC Samples**

Total number of CPVC samples are 60 that are being used in this experiment. Each parameter required 3 samples.

**(iii). CPVC Properties**

**Table 3-3:** Properties of PPR adherend

|          |                      |                            |
|----------|----------------------|----------------------------|
| <b>1</b> | Tensile strength     | 55.16 MPa                  |
| <b>2</b> | Thermal conductivity | 0.24 W/(mK)                |
| <b>3</b> | Specific gravity     | 1.55±0.2 g/cm <sup>3</sup> |
| <b>4</b> | Decomposition point  | 400+ °F                    |

**(iv). Dimensions**

**Table 3-4:** Dimensions of CPVC adherend

|                     |        |
|---------------------|--------|
| CPVC sample length  | 56mm   |
| CPVC outer diameter | 37mm   |
| CPVC inner diameter | 26.7mm |

**3.2.2 Adhesive**

Epoxy Araldite-LY-556 and hardener AD-22962 both used as adhesive material. Epoxy Araldite-LY-556 is brittle in nature as welding, rivets and bolts are being replaced with adhesive joint, it is necessary to use brittle epoxy to make good strength. It is known that brittle material fails easily, so to increase the strength of the joint filler is being added in the epoxy adhesive to prevent crack propagation.

**(a). Epoxy resin**

Any group of polymers which contain epoxide group is called epoxy resin. Epoxy is family of basic components or cured end products of epoxy resin.

**(i). Specification:** Araldite-LY-556

**(ii). Properties**

**Table 3-5:** The properties of epoxy resin

|          |                                |                                 |
|----------|--------------------------------|---------------------------------|
| <b>1</b> | Aspects (Visual)               | Clear Liquid                    |
| <b>2</b> | Viscosity @ 25°C (ISO 12058-1) | 10,000-12,000 [mPa's]           |
| <b>3</b> | Density @ 25°C (ISO 1675)      | 1.15 - 1.2 [g/cm <sup>3</sup> ] |
| <b>4</b> | Epoxies index (ISO 3001)       | 5.30 – 5.40 [Eq/kg]             |

**(b). Hardener**

Hardener is a substance which is added in a specific compound in certain amount. A hardener in solution starts curing process. It acts as reactor or catalyst to strengthen the solution of mixture. It can be referred as an accelerator.

**(i). Specification:** AD-22962

**(ii). Properties:**

**Table 3-6:** Properties of Hardener

|          |                                |                                 |
|----------|--------------------------------|---------------------------------|
| <b>1</b> | Aspects (Visual)               | Colourless little yellow liquid |
| <b>2</b> | Viscosity @ 25°C (ISO 12058-1) | 5-20 [mPa's]                    |
| <b>3</b> | Density @ 25°C (ISO 1675)      | 0.89-0.90 [g/cm <sup>3</sup> ]  |

**(d). Storage**

Both the epoxy resin and hardener are stored in dry ventilated space. Container is tightly sealed that no air enters the container. After taking epoxy resin or hardener contain should be sealed immediately.

### (e). Mix Ratio

**Table 3-7:** Mix ratio for epoxy and hardener

| <b>Components</b> | <b>Parts by Weight</b> | <b>Parts by volume</b> |
|-------------------|------------------------|------------------------|
| Araldite LY-556   | 100                    | 100                    |
| AD-22962          | 23                     | 30                     |

To make the solution, it is preferred to weight accurately to avoid inaccuracies that will affect the matrix system properties. To make the homogenous solution, components of the solution should be mixed properly, first by hand mixing and then preferred to use magnetic stirrer. To avoid inaccuracies in solution, divide the large mixture into small containers.

**Table 3-8:** Adhesive Joints Properties

|                                  |   |
|----------------------------------|---|
| <b>(f). Thickness</b>            | 0.1mm                                       |
| <b>(g). Curing time of epoxy</b> | Cure at 100 °C for 2 hours                  |
| <b>(h).Solution weight</b>       | 10g solution is used for each configuration |
| <b>(i). Application</b>          | Industrial and structural                   |

### 3.2.3 Filler

Cork powder is used as filler in epoxy solution, due to its near non-permeability. Cork stoppers are account about 60% for all cork-based production. Cork has zero poison ratio, means change in radius is not significant when force is applied on it. Filler is made of cork granules in concrete.

**Table 3-9: Properties of Filler**

|          |                      |                               |
|----------|----------------------|-------------------------------|
| <b>1</b> | Density              | 400-1500 [kg/m <sup>3</sup> ] |
| <b>2</b> | Compressive strength | 1-26 [MPa]                    |
| <b>3</b> | Flexural strength    | 0.5-4.0 [MPa]                 |

(i). **0.25wt.%, 0.5wt.%, 0.75wt.%, 1wt.%** are being used in solution to make the tubular adhesive joint.

### **Equipment Utilized**

- 1) Magnetic Stirrer
- 2) Electronic balance
- 3) Universal Testing Machine

#### **1) Magnetic Stirrer**

Magnetic stirrer is device used to mix the solution in lab. It has a rotating plate and a magnet which is covered with the plastic sheet. When plate rotate it produce the magnetic field to rotate the magnet which is placed inside the solution. Rotation of magnet helps to mix the solution. This device also has heater which is used for heating purposes. In this experiment heater is used to make the solution of cork filler and epoxy.



**Figure 3.2: Magnetic Stirrer**

## 2) Electronic balance

Electronic balance is used to weight the chemical in the laboratory. This balance device makes the accurate measurement. In the experiment it is used to make the accurate measurements of epoxy resin, hardener and cork filler. Balance device was able to measure up to 1 milligram.



**Figure 3.3:** Electronic Balance

## Universal Testing Machine

**Table 3-10:** Functional properties of UTM

| Description   | Details  |
|---------------|--|
| Specification | HD-B607-S HAIDA INTERNATIONAL EQUIPMENT CO., LTD   |
| Capacity      | 100KN load cells   |
| Load accuracy | Less than equal to $\pm 0.5\%$   |
| Test in UTM   | In this experiment tensile test under 25-degrees, 50-degrees, 75-degrees, and 100-degrees will be conducted in temperature chamber |

|                 |   |
|-----------------|---|
| Troubleshooting | In case of any emergency press red E button to stop the operation of machine. During testing it is prohibited to touch the machine or heating chamber |
| Operation Mode  | Computer software “TESTER” relates to UTM to control the operation. Results taken manually in excel sheet   |
| Test speed      | 1.0mm/min   |
| Display         | After testing it display maximum failure load, length, time taken and position. Results taken manually in excel sheet                                 |
| Operation       | Testing speed, type of test, length, width is chosen according to requirements  |

### **3.4 Procedure for Manufacturing and testing of tubular adhesive joints.**

The procedure consists of following three steps.

1. Decreasing of steel pipe and polymers
2. Preparation of tubular joints
3. Testing of tubular adhesive joint.

These steps further divided into sub parts which will be explain next.

#### **3.4.1 Decreasing of steel pipes**

Tubular adhesive joint is widely used in construction and industrial applications. The joint making process of tubular joint is more complex than the other joints. It is necessary to clean the adherend material before making joint to increase the strength of the joint. Decreasing is the process of removal unwanted particles from the adherend. Following steps are include in the decreasing of steel pipe.

#### **Step 1. Washing of steel pipes with detergent**



In decreasing process, first step is to wash the steel adherend in washing soda. In this process surface tension act between the grease and water. Also, it is helpful to remove the particles adjusted with the steel pipe. Adherend specimens are placed in the washing soda for 15 mins, so that all the grease material will be removed. After removing from the detergent, it is cleaned with the water and place it for to dry. It is advisable to use gloves during washing because sharp edges can make injury.

### **Step 2. Clean the surface with sandpaper.**

After removing the grease and dust particles from the surface of the steel pipes, sandpaper used to remove the course marks, or region on the surface by using medium size grid of 100 and then fine grit size of 200 to make the surface smooth. After using sandpaper, it was cleaned again with detergent to remove the dust particles from the surface.

### **Step 3. Clean the surface with Acetone.**

Acetone is required for a variety of purposes including dust removal, decreasing, finishing and for paint removal. Acetone is favourable in case of removing the dust and greasing from the surface when very high accuracy is required in the results. In process of decreasing the steel pipes, first marks the region which is required to make joint, and adhesive will be used. Fill the beaker to that level and dip the steel pipe specimens in the beaker. Place that specimen for 10 minutes and applied the water break test, surface did not pass the water break test and then place for 5 more minutes in acetone and then apply the water break test to see that surface become smooth. It is required because in water break test, duration of placing the specimen in acetone is obtained. After placing the steel specimen in the beaker, it is required to close the beaker because acetone is highly volatile.



**Figure 3.4:** Cleaning steel surface with acetone

#### **Step 4. Water break test**

Water break test used to check the cleanliness of the surface from contaminants. After placing the steel sample in acetone water break test is to see the cleanness of the surface. If the water break into droplets, then the surface contained the contaminants. In our case, there were no droplets after placing the steel specimen in acetone for 15 minutes.

#### **3.4.2. Decreasing of Polymers specimens.**

The process of decreasing the polymer specimen includes 2 steps. It includes washing the polymer specimen in detergent and then using the fine sandpaper to make the surface smooth. As the polymer sockets which used is already smooth. Whereas in case of PPR sockets, internal removing of material was done through lathe machine. Although this process maintains the smooth surface, but it was as before material removal.

- (i). In first step place the PPR and CPVC sockets specimen in detergent separately and clean it to remove the grease and dust particles.
- (ii). Extra fine Sandpaper used in case of PPR sockets to make the surface smooth.

#### **3.4.3. Preparation of neat Tubular Joint**

In preparation of neat tubular joint epoxy and hardener are mixed without filler in the mixture. As neat adhesive takes less time to prepare as compared to adhesive with filler concentration. We prepared 12 joints for PPR socket and 12 joint for CPVC. Three samples against every temperature. Temperature ranges are 23, 50, 75, and 100 degrees.

### 3.4.4. Mixing of Epoxy and Hardener

Epoxy is composed of resin and hardener. Combining the resin and hardener chemical reaction is occur which makes the liquid epoxy to hard. A special ratio and accurate measurement are used to make the epoxy cure properly. Following steps applied to make the measurements and mixing of epoxy resin.

- 1) Calculate the amount of epoxy resin required.
- 2) Calculate the amount of Epoxy and resin required.
- 3) Accurately measure the amount the Epoxy and hardener.
- 4) Adequate mixing of epoxy and hardener.

After taking the epoxy and hardener, it is necessary to close the binder clips, so no curing process start.

#### Step 1. Calculate the epoxy resin required.

We have taken 100:23 portion of epoxy: hardener. It means for 100 parts of epoxy 23 parts of hardener are taken. We have prepared 10g of solution for every configuration. So the amount of epoxy and hardener taken are shown in following equation.

$$E:H = 100: 23$$

$$\text{Amount of epoxy in 10g of solution} = 10g * \left(\frac{100}{123}\right) = 8.13g$$

$$\text{Amount of hardener} = 10g * \left(\frac{23}{123}\right) = 1.87g$$

So, amount of epoxy required is 8.13g while hardener is 1.87g.

#### Step 2. Measure of epoxy and hardener

- (i). Take a 100ml beaker. Electronic weight device is used for accurate measurement. As the desire amount is in gram, set the scale in grams.
- (ii). Place the beaker on the weight device and measure the weight of the beaker. The press the tare button to make the reading to zero.
- (iii). Take the epoxy and start pouring it in the beaker slowly to get the amount of 8.13 gram in beaker.
- (iv). If higher amount is poured in the beaker, it can be removed by the help of spatula.

- (v). Once the epoxy has been added to the beaker, now time to pour the hardener in the beaker. Tare the weight of the beaker to zero and start pouring 1.87g of hardener.



**Figure 3.5:** Weight measurement for epoxy and hardener

### **Step 3. Adequate Mixing**

The following steps are taken for adequate mixing of the mixture.

- (i). After adding the right proportion of epoxy and hardener, it is required to simply mix using spatula for 5 minutes. Increase the time if a higher amount is being mixed.
- (ii). Scrape the corner and sides of the beaker during mixing for coherent mixing to avoid any improper curing.
- (iii). Used the magnetic stirrer for appropriate mixing for about 15 minutes at higher rpm. After mixing using stirrer, again mix the solution for 2-3 minutes.



**Figure 3.6:** Stirring of epoxy adhesive on magnet stirrer.

### **3.4.5. Joining the Steel pipes and PPR socket**

- (i). After mixing the epoxy and hardener. Covered the table with sheet, so that epoxy does not stick with table.
- (ii). Uncover the steel and PPR pipes specimens. To make the joint of steel and PPR pipe
- (iii). Start applying the epoxy on the inner side of the PPR socket to length of 26.7mm.
- (iv). Apply the epoxy on both steel pipe specimens on outer side of the pipe to required length of 26.7mm.
- (v). After properly applying the epoxy on both steel specimens and PPR socket. Take the Steel pipe specimen and put it inside the socket to make the joint. Again, take the steel pipe and put inside on the other side of the socket.
- (vi). Checked the alignment of holes on both steel pipes attached to the PPR socket.



**Figure 3.7** Adhesive joints of steel and PPR pipes at different cork concentrations

#### **3.4.6. Curing the joints in oven**

- (i). Life the epoxy is two hours, after making joint, placed them inside the oven for curing.
- (ii). Close the door of oven and turn on. Set the value of temperature for curing for 100 degrees.
- (iii). After reaching the temperature of 100 degrees on the oven, set the timer for two hours to cure it.
- (iv). After two hours, turn off the oven and open the door. Let the cool down oven to room temperature. Now the joints cool down, remove the joints.
- (v). Now the joints without filler concentration are prepared.



**Figure 3.8:** Curing of joints in oven at 100 degrees temperature

### **3.4.7. Preparation of Tubular joints with filler concentration**

In preparation of tubular adhesive joints filler is added with epoxy first and mixing it with Capula for 5 minutes to make epoxy and cork filler homogenous. Filler works as sealing agent and increase the overall strength of the joint. Filler is added in the proportion of 0.25%, 0.50%, 0.75% and 1% in the solution. 10g solution is prepared along every configuration.

### **3.4.8. Mixing of epoxy resin, hardener, and cork filler**

In process of mixing the epoxy and cork filler. Make the measurements for epoxy and cork filler. Mix it manually first with Capula for 5 minutes to make it homogenous. After mixing it manually, mixture of epoxy resin and cork filler is stirrer up using magnetic stirrer for 20 minutes with heating at 50 degrees temperature to make the solution completely homogenous.

After mixing at magnetic stirrer, wait for 10 minutes to cool down the solution. After cooling down mixture of epoxy resin and cork filler, next step is to add the hardener. Epoxy is

composed of resin and hardener. Combining the resin and hardener chemical reaction is occur which makes the liquid epoxy to hard. A special ratio and accurate measurement are used to make the epoxy cure properly. Following steps applied to make the measurements and mixing of epoxy resin.

- 1) Calculate the amount of epoxy resin, hardener and cork filler required.
- 2) Adequate mixing of epoxy resin and cork filler.
- 3) Adequately mixing of solution of epoxy resin and cork filler with hardener.

### **Step 1. Calculate the epoxy resin, hardener and cork filler required.**

We have taken 100:23 portion of epoxy: hardener. It means for 100 parts of epoxy 23 parts of hardener are taken. We have prepared 10g of solution for every configuration. So, the amount of epoxy and hardener taken are shown in following equation.

$$E:H = 100: 23$$

$$\text{Amount of epoxy in 10g of solution} = 10g * \left(\frac{100}{123}\right) = 8.13g$$

$$\text{Amount of hardener} = 10g * \left(\frac{23}{123}\right) = 1.87g$$

So, amount of epoxy required is 8.13g while hardener is 1.87g.

The amount of the filler will be 0.25% or 0.0025 of the solution.

### **Step 2. Measure of epoxy and cork filler**

- (i). Take a 100ml beaker. Electronic weight device is used for accurate measurement. As the desire amount is in gram, set the scale in grams.
- (ii). Place the beaker on the weight device and measure the weight of the beaker. The press the tare button to make the reading to zero.
- (iii). Take the epoxy and start pouring it in the beaker slowly to get the amount of 8.13 gram in beaker.
- (iv). If higher amount is poured in the beaker, it can be removed by the help of spatula.
- (v). Once the epoxy has be added to beaker, now time to add the filler an amount of 0.25% of solution.
- (vi). Mixed for 3-5 minutes with spatula.



- (vii). Turn on the magnet stirrer and heater to heat the epoxy and filler for 15 minutes to make the homogenous solution.
- (viii). Monitor the temperature, so that it will not increase more than 50 degrees. When temperature reached 35 degrees, turn off the heater as it goes increasing after that due to heated plate.
- (ix). After mixing, wait for to decrease the temperature to room temperature.
- (x). Add the hardener into the solution of epoxy and filler. Mix for 5 minutes and use magnet stirrer to mix homogeneously.
- (xi). Avoid adding the hardener into the epoxy at elevated temperature, otherwise hardener will react with the epoxy and make it hard immediately.

### **Step 3. Adequate Mixing**

The following steps are taken for adequate mixing of the mixture.

- (i). After adding the right proportion of epoxy and hardener, it is required to simply mix using spatula for 5 minutes. Increase the time of higher amount is being mixed.
- (ii). Scrape the corner and sides of the beaker during mixing for coherent mixing to avoid any improper curing.
- (iii). Used the magnetic stirrer for appropriate mixing for about 15 minutes at higher rpm. After mixing using stirrer, again mix the solution for 2-3 minutes.
- (iv). Now make the joints by applying the adhesive on inner side of the PPR and outer side of the steel specimen. This procedure is repeated as explained earlier.
- (v). Process of making the solution for 0.50%, 0.75 and 1% is repeated as stated above.

### **3.4.9. Testing of Tubular Adhesive Joint**

When joints are prepared, testing of tubular adhesive joint involve tensile testing on universal testing machine (UTM). Fixtures were prepared to fix the joint in UTM. Fixtures were manufactured with stainless steel to bear tensile testing. These fixtures were fixed with the UTM fixtures to fix the specimens for tensile testing.

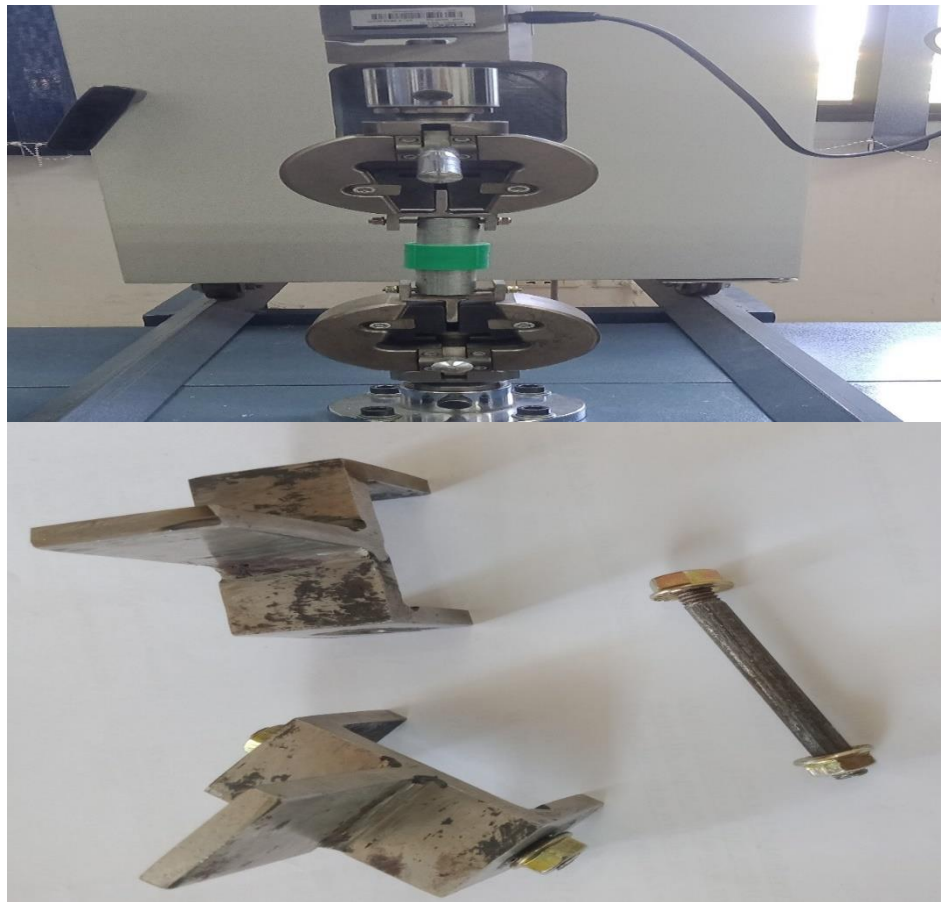


**Figure 3.9:** Fixtures for tubular specimens

This testing involves finding the strength of the joint between adhesive and adherend. Yield point is where proportional limit ends. Ultimate tensile point where joint break off. 100 KN sensor is attached with the UTM. In this testing temperature for each configuration is done at 25, 50, 75, 100 degrees.

#### **3.4.10. Testing of Tubular Joints at 25 degrees.**

Testing involves following steps.

- (i). Turn on the UTM machine, TESTER software which is installed in computer.
- (ii). Set up the dimensions for specimen using TESTER to move the fixture upward.
- (iii). Fixed the fixtures made up for tubular joint to fix the tubular joint in fixtures of UTM.
- (iv). Fixed the tubular specimen and applied preload on the joint to start testing.
- (v). Speed of testing is maintained at 1mm/min for all tests.
- (vi). Start the testing to get the result of load against length of the specimen of joint.
- (vii). As the test start a graph showing values of load against length is continuously showing. Which show the behaviour of joint.

- (viii). It is advisable that do not touch the UTM during the testing to save from any error in testing.
- (ix). As the specimen break off. Either the UTM automatically stop or by manual to get the results.
- (x). Initial result which shows is max load against max length of the specimen along the graph.
- (xi). After the testing is stop, immediately save the results file by clicking on menu then save the file with name of #sample\_1 to save any chance of lost or TESTER software sometime restart due to loading.
- (xii). Now go on calculate data and click on tensile test data. As the values shown on screen, click any value and press control A to select all values and then control C to copy data.
- (xiii). Opened the excel file and paste the data and save excel file. Every sheet given special name to make difference with results.
- (xiv). Remove the specimen after testing is completed for specimen.
- (xv). Repeat the process for 2<sup>nd</sup> specimen for same temperature. Also, for specimen with filler concentration of 0.25%, 0.50%, 0.75% and 1%.

#### **3.4.11. Testing of Tubular Joints at 50 degrees.**

Testing specimens with temperature more than 25 degrees required temperature chamber (Oven) with is attached with UTM through stand and can be move towards UTM through rails. Remove the first attached fixture with UTM and move the temperature chamber towards UTM, as it move to the required place fix the fixtures according to the requirement and load cell of 100 KN according to design of temperature chamber.

- (i). Turn on the UTM and TESTER to run the UTM setup.
- (ii). Fix the specimen in the chamber and applied the preloading.
- (iii). Turn on the temperature chamber and set the temperature 50 degrees manually. Wait for that temperature to reach 50 degrees.
- (iv). As the temperature is reached, start testing, results of load against length will be shown on the screen.
- (v). After the testing is stop, immediately save the results file by clicking on menu then save the file with name of #sample\_ to save any chance of lost or TESTER software sometime restart due to loading.

- (vi). Now go on calculate data and click on tensile test data. As the values shown on screen, click any value and press control A to select all values and then control C to copy data.
- (vii). After data is saved, retrieved that preload and remove the specimen for next testing.

### **3.4.12. Testing of Tubular Joints at 75 and 100 degrees.**

For testing at 75- and 100-degrees process remains same as for 50 degrees. Manually changed the temperature.

- (i). Turn on the temperature chamber and wait for to reach the required temperature.
- (ii). Start the test to get the results and data.
- (iii). Repeat the process to save the file.

Results of all the specimens are discussed in detail in next section.



**Figure 3.10:** Adhesive joint during testing at 100 degrees temperature

## Chapter 4: Results and Discussion

### 4.1. Effect of temperature and cork powder on failure load of tubular adhesive joint for CPVC and Steel:

The tubular adhesive joint with CPVC and steel adherend at four different temperatures of 25, 50, 75 and 100 degrees is experimented to evaluate the failure load with and without cork powder concentration. Cork powder concentration from 0.25 wt.%, 0.5 wt.%, 0.75 wt.% and 1 wt.%. Three samples were tested against each configuration with displacement rate of 1.5mm/min. Average failure load against each temperature and each concentration was recorded after tensile testing.

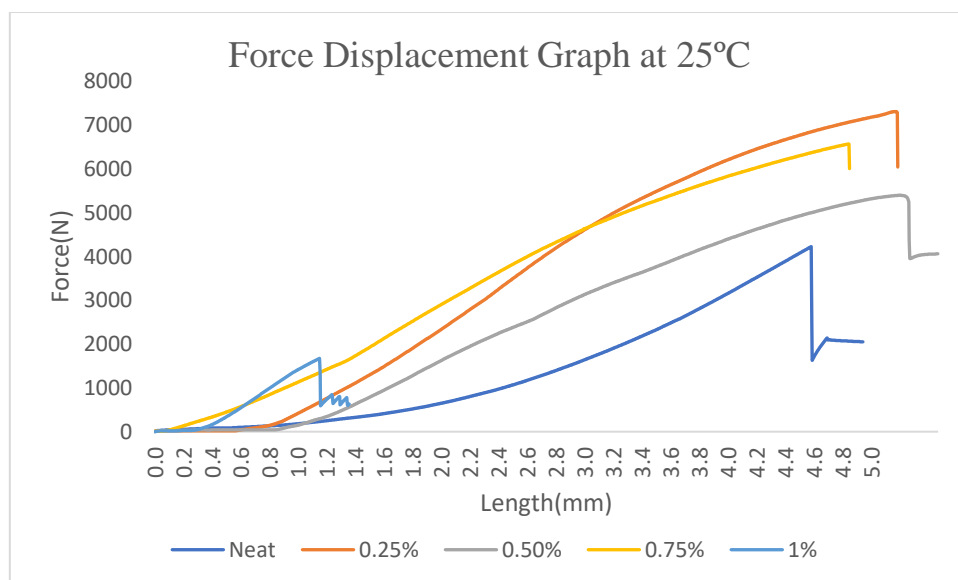
Fig. 4.1 illustrate the failure load and displacement graph with and without cork powder concentration of 0.25 wt.%, 0.5 wt.%, 0.75 wt.% and 1 wt.% at 25-degree temperature. The results show that failure load is increased with the cork powder of 0.25 wt.% and then decreases from 0.5 wt.% till 1 wt.%. Highest failure load is recorded for 0.25 wt.%. Neat adhesive failure load is recorded at 4.22KN with displacement of 1.2mm. 0.25 wt.% cork concentration failure load is recorded at 7.32KN with displacement of 5.2mm while 5.39KN failure load was recorded for 0.5 wt.% against displacement of 5.49mm. Failure load for 0.75 wt.% concentration was recorded 6.56KN with displacement of 4.87mm. Lowest failure load recorded for 1 wt.% cork concentration with value of 2.30KN force. The strength of the tubular adhesive joint increases from neat to 0.25 wt.% and then decreases from 0.50 wt.% to 1 wt.% cork concentration at 25 degrees.

Figure 4.2 shows the failure load and displacement graph with and without cork powder concentration of 0.25 wt.%, 0.5 wt.%, 0.75 wt.% and 1 wt.% at 50-degree temperature. Results shows that maximum failure load at 7.43KN with displacement of 7.9mm was achieved with cork powder concentration of 0.25 wt.%. Failure load without cork concentration was seen lowest with value of 1.44KN with displacement of 2mm. Failure load of 5.37KN with displacement of 6mm having cork concentration of 0.50 wt.% was seen which start decreasing after 0.25 wt.%. 6.12KN failure load was seen with cork concentration of 0.75 wt.% and displacement of 4.7mm. Failure load of adhesive joint with cork concentration of 1 wt.% was very linear with value of 3.03KN as compared to other joints with displacement of 5.5mm.

Fig 4.3 shows the failure load and displacement graph with and without cork powder concentration of 0.25 wt.%, 0.5 wt.%, 0.75 wt.% and 1 wt.% at 75-degree temperature. The

maximum failure load was recorded at 5.56KN with displacement of 0.9mm with cork concentration of 0.75 wt.%. Lowest failure load recorded for 1% cork concentration with failure load 1.06KN with displacement of 0.3mm. Failure load increased from 0.25 wt.% to 0.75 wt.%. Failure load for 0.25 wt.% cork concentration was recorded 3.98KN with displacement of 1.1mm. Failure load for 0.50 wt.% cork concentration was recorded 4.55KN with displacement of 0.7mm. While the failure load for 0.75 wt.% concentration was recorded with value of 5.49KN with displacement of 0.9mm.

Fig 4.4 shows the failure load and displacement graph with and without cork powder concentration of 0.25 wt.%, 0.5 wt.%, 0.75 wt.% and 1 wt.% at 100-degree temperature. The increase in failure load from neat adhesive to 0.75 wt.% concentration of cork powder was recorded in experiment. Failure load for neat adhesive recorded with value of 1.74KN with displacement of 1.9mm. Then increase in failure load recorded for 0.25 wt.% cork concentration with value of 3.09KN and displacement of 3mm. The further increase in failure load was recorded for 0.50 wt.% cork concentration with value of 3.7KN with displacement of 3mm. The highest value of failure load of 4.76KN recorded for 0.75 wt.% cork concentration with displacement of 5mm. Lowest value of failure load recorded for 1 wt.% cork concentration with value of 1.37KN with displacement of 1.3mm.



**Figure 4.1:** Force displacement curve at 25°C temperature and at different concentration

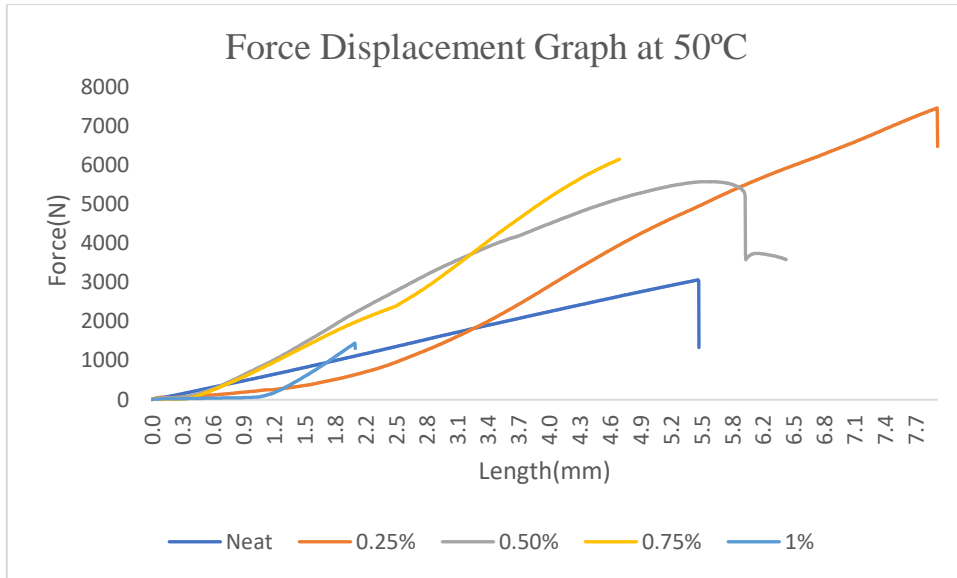


**Figure 4.2:** Force displacement curve at 50°C temperature and at different concentration

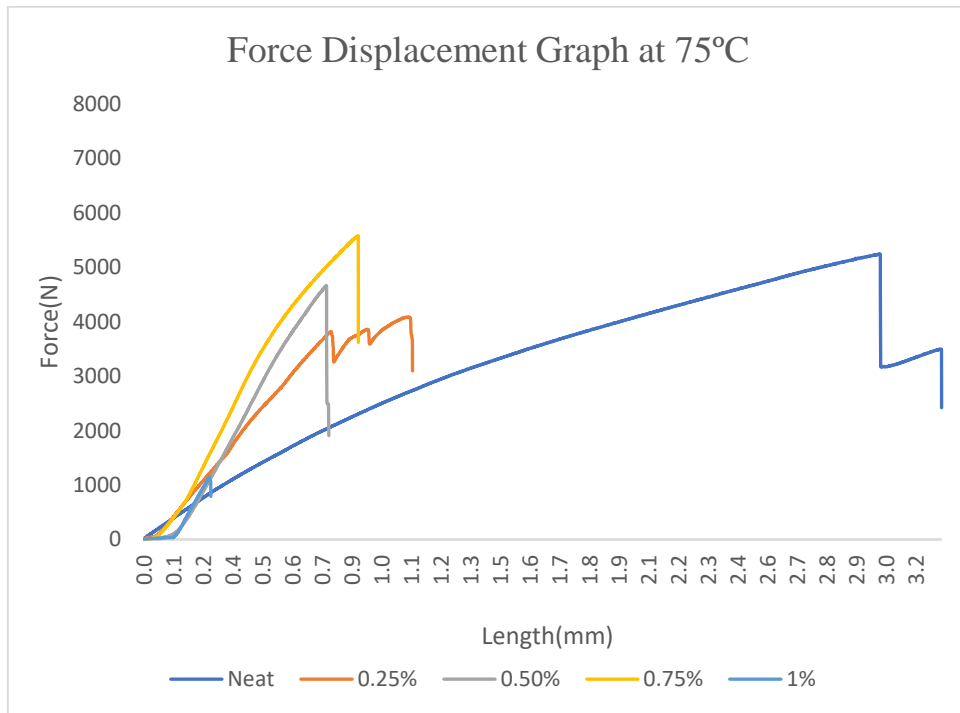


**Figure 4.3:** Force displacement curve at 75°C temperature and at different concentration

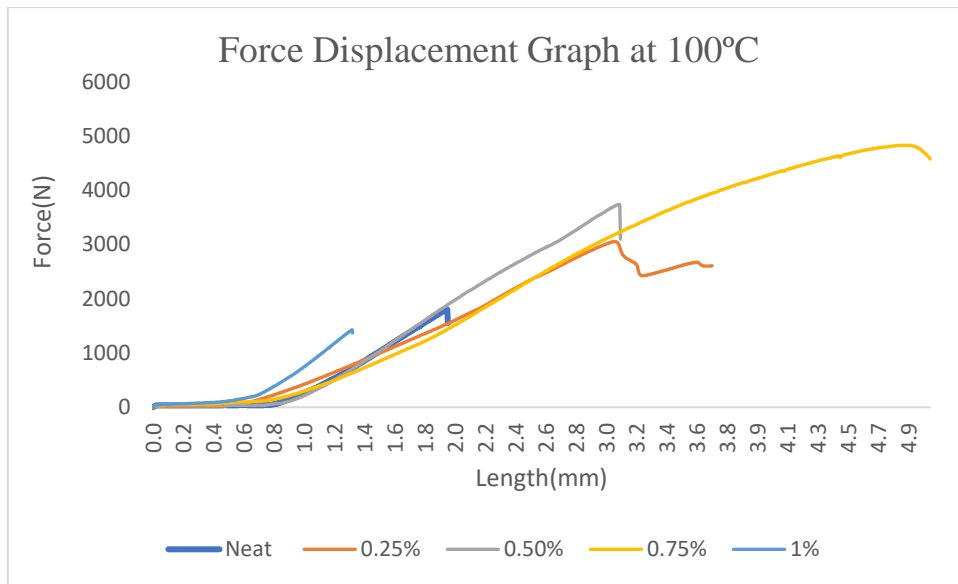


**Figure 4.4:** Force displacement curve of tubular joint at 100°C temperature and at different concentration

There were three samples that were tested against each configuration of joint with displacement rate of 1.5mm/min. The average failure load values were recorded at temperatures of 25°C, 50°C, 75°C and 100°C and at cork concentration of 0.25 wt.%, 0.5 wt.%, 0.75 wt.% and 1 wt.%.

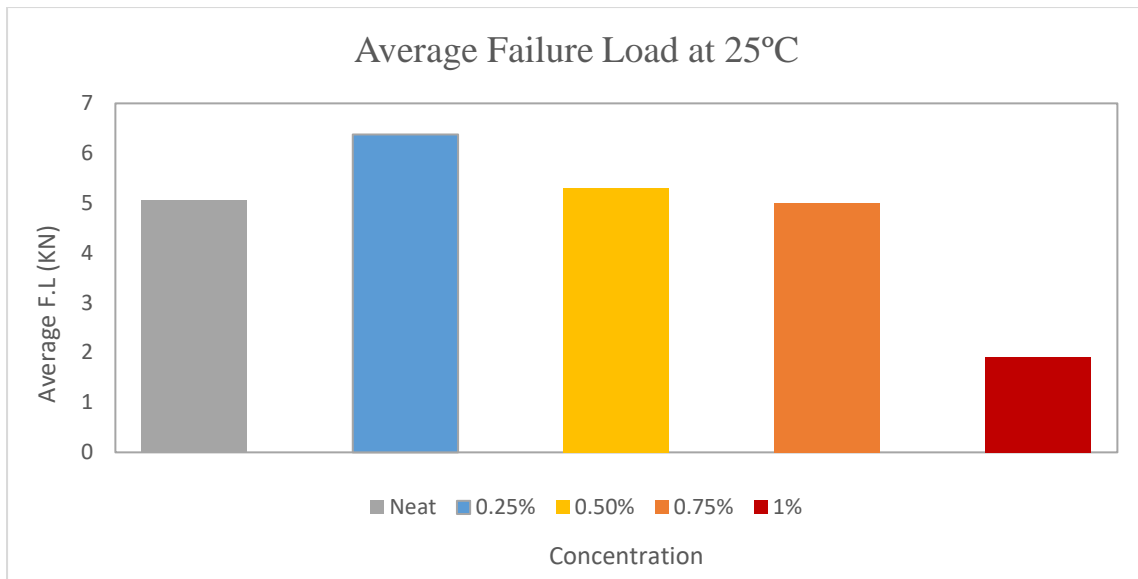
Fig 4.5. shows the average failure load of tubular joint for different cork concentration of 0.25 wt.%, 0.5 wt.%, 0.75 wt.% and 1 wt.% and at 25°C temperature. The highest average failure load recorded for cork concentration of 0.25 wt.% with value of 6.37KN. First the average failure load increases from neat adhesive to 0.25 wt.% cork concentration and then start decreases from 0.5 wt.% to 1 wt.% cork concentration. The average failure load of neat joint is 5.06KN, while the average failure load for 0.5 wt.% is 5.29KN. 5.29KN failure load is recorded for 0.50 wt.% cork concentration. Cork concentration of 0.75 wt.%, average failure load is recorded at value of 4.99KN. The lowest value of average failure load recorded for 1 wt.% cork concentration of 1.92KN.



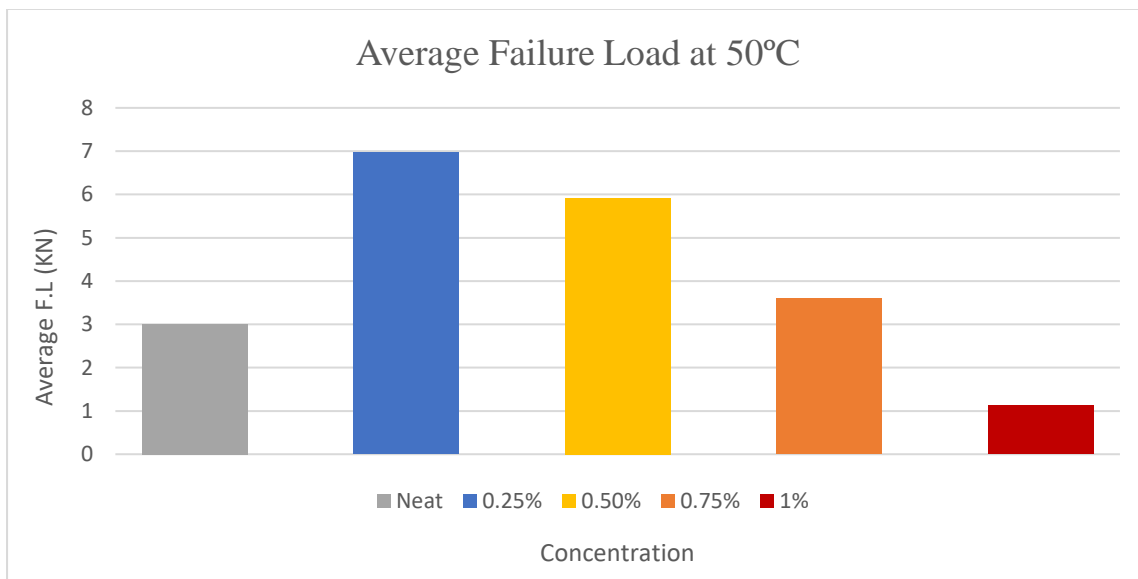
Fig 4.6 shows the average failure load at 50°C temperature and cork concentrations of 0 wt.%, 0.25 wt.%, 0.5 wt.%, 0.75 wt.% and 1 wt.%. First the average failure load increase from neat adhesive joint to 0.25 wt.% concentration and then start to decrease till 1 wt.%. The highest average failure load recorded at 6.97KN with cork concentration of 0.25 wt.%. Average failure load for 0.5 wt.% recorded 5.91KN. 3.59KN average failure load recorded for 0.75 wt.%. The average failure load for 1 wt.% recorded at 1.12KN which is the lowest average failure load. 3KN average failure load recorded for neat adhesive joint.

Fig 4.7 shows the average failure load at 75°C temperature and cork concentrations of 0.25 wt.%, 0.5 wt.%, 0.75 wt.% and 1 wt.%. The increase in average failure load was recorded from neat joint to 0.5 wt.% concentration and then start to decrease till 1 wt.%. The average failure for neat adhesive recorded is 3.42KN, for 0.25 wt.% cork concentration the recorded average failure load is 4.68KN. The highest average failure load recorded for 0.5 wt.% cork concentration is 4.88KN. 3.94KN average failure load recorded for 0.75 wt.% cork concentration. Lowest average failure load recorded 0.94KN with cork concentration of 1 wt.%.

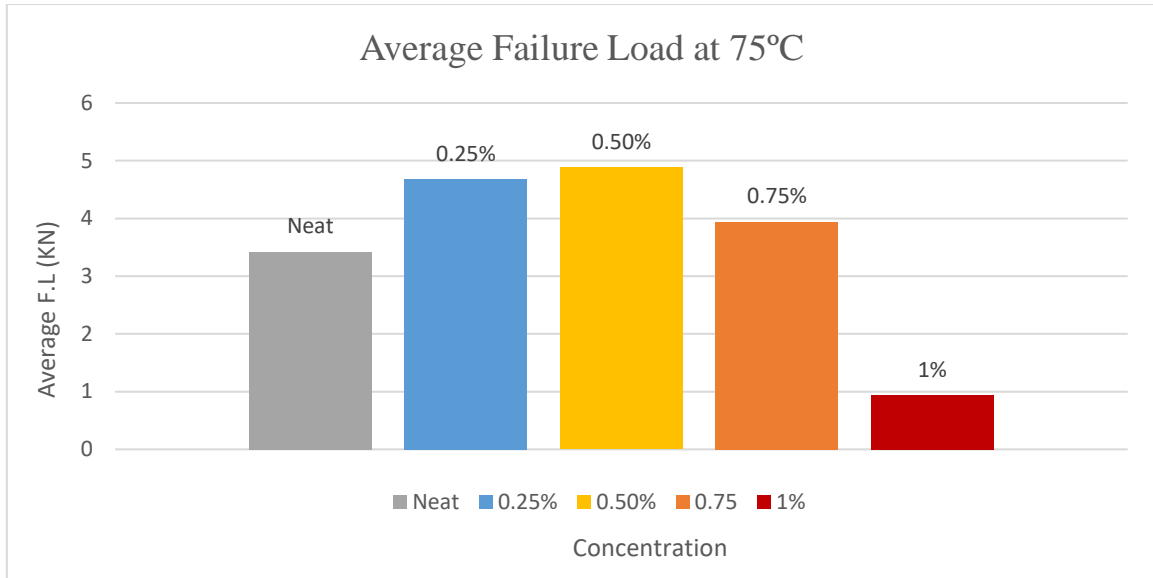
Fig 4.8 shows the average failure load at 75°C temperature and cork concentrations of 0.25 wt.%, 0.5 wt.%, 0.75 wt.% and 1 wt.%. The average failure load increased from neat adhesive joint to 0.5 wt.% adhesive joint. 1.49KN average failure load recorded for neat adhesive, for 0.25 wt.% cork concentration the average failure load recorded is 3.63KN. The highest failure load recorded for 0.5 wt.% is 4.03KN. For 0.75 wt.% the average failure load recorded is 3.38KN. The lowest average failure load recorded for 1 wt.% cork concentration is 0.70KN.



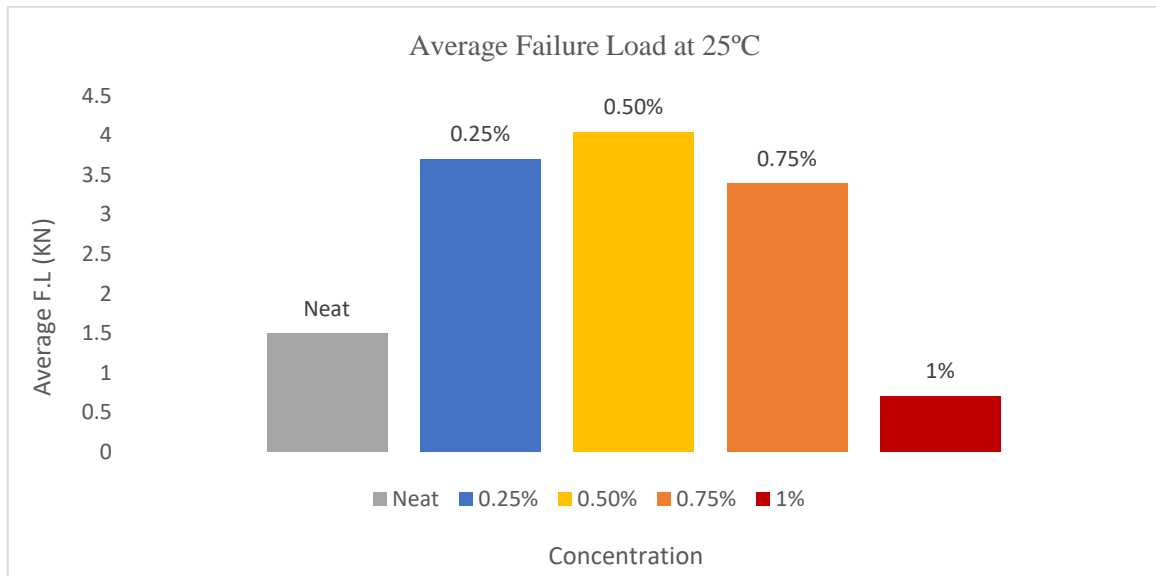
**Figure 4.5:** Average failure load of tubular joint at 25 °C and at different cork concentrations



**Figure 4.6:** Average failure load of tubular joint at 50°C and at different cork concentrations



**Figure 4.7:** Average failure load of tubular joint at 75°C and at different cork concentrations



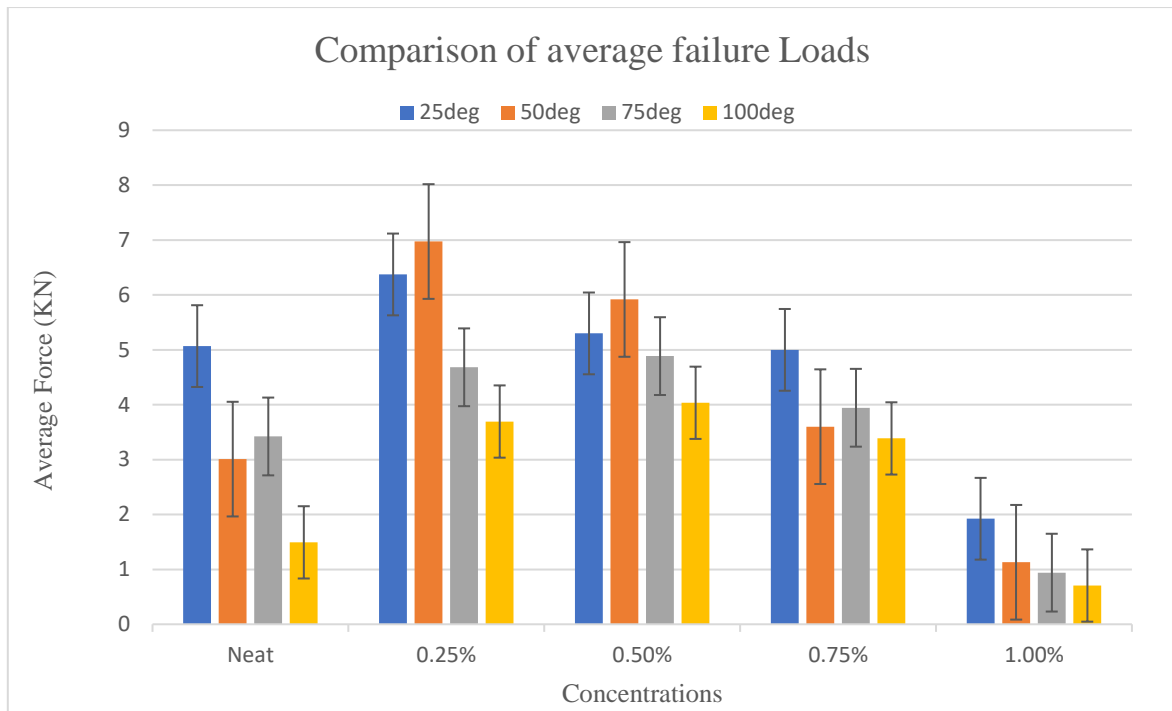
**Figure 4.8:** Average failure load of tubular joint at 100°C and at different cork concentrations

Table 4.1 shows the average failure load at different concentrations and at different temperatures. For neat adhesive the highest average failure load was recorded at 25°C and start to decrease as the temperature increases. The lowest failure load was recorded at 100°C for neat adhesive. We can say that as the temperature increases the strength of the joint decreases for neat adhesive. Result data for 0.25 wt.% recorded highest average value as compared to other concentrations. As the cork concentration increases from 0.50 wt.% to 1 wt.% the average failure load decreases due to change in properties of the adhesive joint. For 0.25 wt.% cork concentration the highest average failure load recorded at 50°C temperature. As the temperature of the joint increases the average failure load decreases. This is due to changes in properties of the joint with increases in temperature. Average failure load for concentrations for neat and from 0.50 wt.% to 1 wt.% decreases with the increase in temperature. The lowest values of average failure load achieved for 1 wt.% cork concentration. The values decrease from 25°C to 100°C. It can be concluded that in general the strength of the joint decreases with the increase in cork concentration and with increase in temperature.

Fig 4.9 shows the comparison of average failure load at different cork concentrations and different temperature.

**Table 4-1:** Average failure load at different concentrations and at different temperatures

| Serial No. | Concentration | Average F.L at 25°C in KN | Average F.L at 50°C in KN | Average F.L at 75°C in KN | Average F.L at 100°C in KN |
|------------|---------------|---------------------------|---------------------------|---------------------------|----------------------------|
| 1          | Neat          | 5.06                      | 3.0                       | 3.42                      | 1.49                       |
| 2          | 0.25 wt.%     | 6.37                      | 6.9                       | 4.68                      | 3.6                        |
| 3          | 0.50 wt.%     | 5.29                      | 5.91                      | 4.8                       | 4.03                       |
| 4          | 0.75 wt.%     | 4.99                      | 3.59                      | 3.94                      | 3.38                       |
| 5          | 1 wt.%        | 1.92                      | 1.12                      | 0.94                      | 0.7                        |



**Figure 4.9:** Comparison of average failure load at different temperatures and at different concentrations.

**Table 4-2:** Failure load comparison at different temperatures and at different concentrations with reference to room temperature.

| Concentration | Temperature | Effect (%) |
|---------------|-------------|------------|
| Neat          | 25°C        |            |
|               | 50°C        | -68.4246   |
|               | 75°C        | -48.1099   |
|               | 100°C       | -239.634   |
| 0.25 wt.%     | 25°C        |            |
|               | 50°C        | 8.600249   |
|               | 75°C        | -36.1364   |
|               | 100°C       | -72.5697   |
| 0.50 wt.%     | 25°C        |            |
|               | 50°C        | 10.45516   |
|               | 75°C        | -8.4681    |
|               | 100°C       | -31.3176   |
| 0.75 wt.%     | 25°C        |            |
|               | 50°C        | -38.874    |
|               | 75°C        | -26.7388   |
|               | 100°C       | -47.6519   |
| 1 wt.%        | 25°C        |            |
|               | 50°C        | -70.1889   |
|               | 75°C        | -104.396   |
|               | 100°C       | -172.238   |

**Table 4-3:** Failure load comparison of neat with different cork concentrations at different temperatures

| Temperature | Concentration (wt.%) | Effect (%)   |
|-------------|----------------------|--------------|
| 25°C        | 0                    |              |
|             | 0.25                 | 20.48747319  |
|             | 0.50                 | 4.365878208  |
|             | 0.75                 | -1.366940055 |
|             | 1                    | -163.6489768 |
| 50°C        | 0                    |              |
|             | 0.25                 | 56.85055933  |
|             | 0.50                 | 49.15502479  |
|             | 0.75                 | 16.41818687  |
|             | 1                    | -166.4108619 |
| 75°C        | 0                    |              |
|             | 0.25                 | 26.91540872  |
|             | 0.50                 | 29.96247015  |
|             | 0.75                 | 13.25952844  |
|             | 1                    | -263.842609  |
| 100°C       | 0                    |              |
|             | 0.25                 | 59.59924181  |
|             | 0.50                 | 63.02354399  |
|             | 0.75                 | 55.93186965  |
|             | 1                    | -111.3314448 |

## **4.2 Effect of temperature and cork powder on failure load of tubular adhesive joint for PVC and Steel:**

The tubular adhesive joint with PVC and steel adherend at four different temperatures of 25,50,75 and 100 degrees is experimented to evaluate the failure load with and without cork powder concentration. Cork powder concentration from 0.25 wt.%, 0.5 wt.%, 0.75 wt.% and 1 wt.% was used. Three samples were tested against each configuration with displacement rate of 1.5mm/min. Average failure load against each temperature and each concentration was recorded after tensile testing.

Fig 4.10 illustrates the failure load and displacement graph with and without cork powder concentration of 0.25 wt.%, 0.5 wt.%, 0.75 wt.% and 1 wt.% at 25-degree temperature. Results shows that failure load decreases from neat adhesive joint to 1wt.% cork concentration. It can be seen from the graph that failure load is maximum for neat solution with the value of 2.024KN and 2.9mm displacement. Value for 0.25wt.% decreases when compared with neat solution and got failed at 1.458KN with displacement of 2.7mm. It has been recorded that with the increase in cork concentration the value of failure load decreases at same temperature. The lowest value recorded for 1wt.% cork powder and failed at 0.853KN with displacement of 0.9mm. The failure value recorded for 0.5 wt.% is 1.212KN and displacement of 2.1mm. The failure load recorded for 0.75 wt.% is 0.933KN with displacement of 1.1mm. So, it can be concluded that cork concentration has negative effect on the strength of tubular PVC and steel at 25 degrees temperature.

Fig. 4.11 illustrated failure load and displacement graph with and without cork concentrations of 0.25 wt.%, 0.5 wt.%, 0.75 wt.% and 1 wt.% at 50°C temperature. Results shows that the failure load decreases from 0.25 wt.% to 1 wt.% cork concentration. Maximum failure load recorded for neat adhesive with value of 1.049KN with displacement of 1mm. The failure load for 0.25 wt.% cork concentration is 0.965KN with displacement of 2.4mm. The failure load for 0.50 wt.% cork concentration were recorded 0.507KN with displacement of 0.6mm which is lower than 0.25 wt.%. The recorded failure load for 0.75 wt.% was 0.397KN with displacement of 0.7mm. The lowest failure load recorded for 1 wt.% with value of 0.279KN with displacement of 0.2mm.

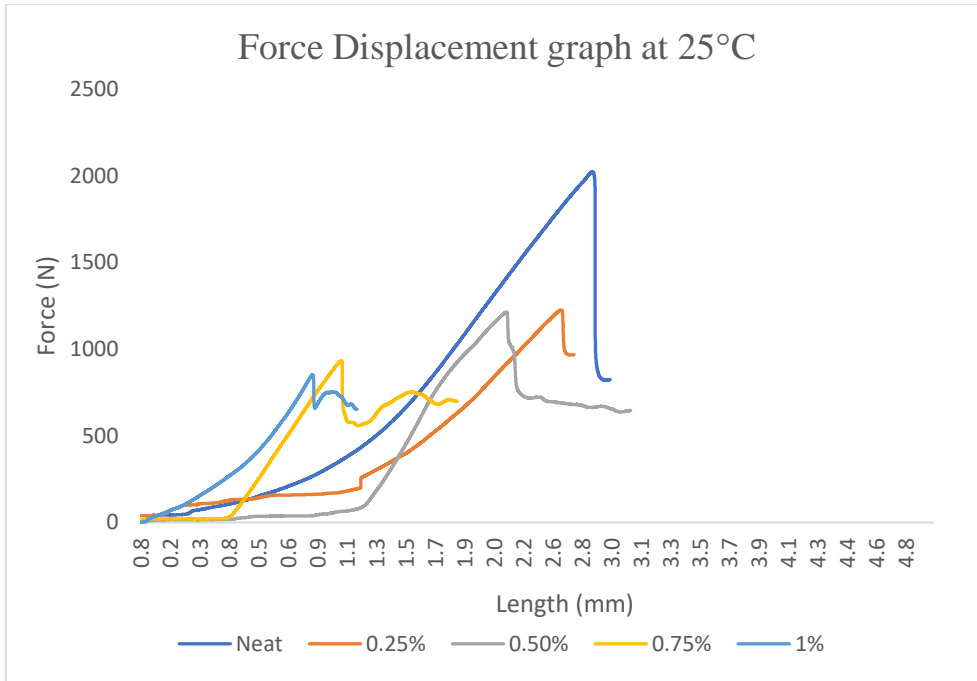
Fig 4.12 exhibited failure load and displacement graph with and without cork concentrations of 0.25 wt.%, 0.5 wt.%, 0.75 wt.% and 1 wt.% at 75°C temperature. Failure is highest for neat solution recorded value of 0.531KN with displacement of 1.1mm. Failure load decreases with



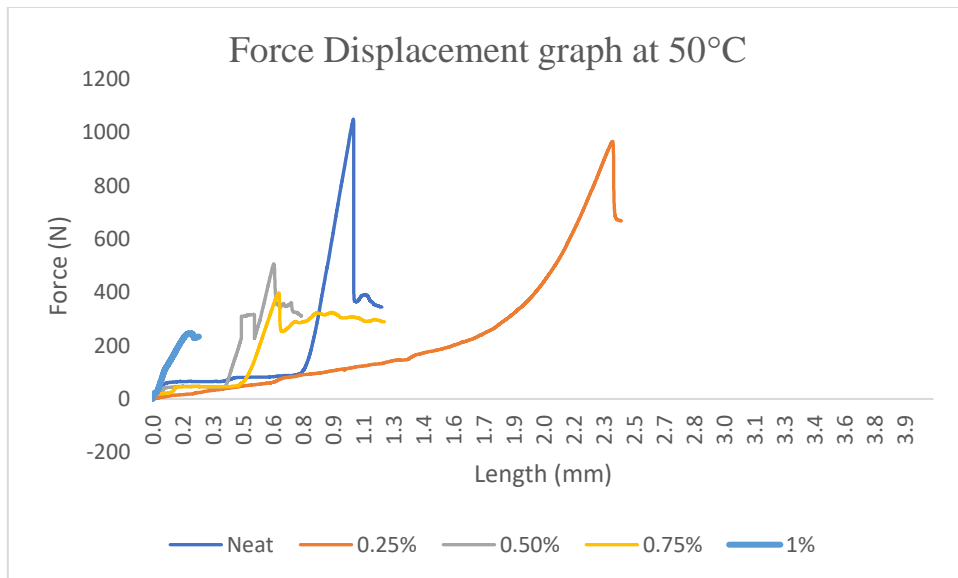
increase in cork concentration. The recorded failure load for 0.25 wt.% was 0.331KN with displacement of 0.5mm. 0.304KN failure load was recorded for 0.50 wt.% with displacement of 0.5mm. The failure load for 0.75 wt.% was lower than 0.5 wt.% and recorded failure load was 0.277KN with displacement of 0.1mm. The lowest failure load recorded for 1 wt.% with recorded value of 0.192KN with displacement of 0.4mm. It can be concluded that with increase in value of cork concentration and at same temperature the strength of joint decreases.

Fig 4.13 illustrated the failure load and displacement graph with and without cork concentrations of 0.25 wt.%, 0.5 wt.%, 0.75 wt.% and 1 wt.% at 75°C temperature. Graph shows that maximum failure load recorded for neat solution with value of 0.5KN with displacement of 3.1mm. The failure load values decrease from 0.25wt.% to 1 wt.%. The failure load recorded for 0.25 wt.% with value of 0.228KN with displacement of 4.2mm. 0.18KN failure load was recorded for 0.50 wt.% with displacement of 1.2mm. The failure load for 0.75 wt.% was recorded with value of 0.152KN with displacement of 0.3mm. The lowest recorded value of failure load was 1 wt.% cork concentration with value of 0.137KN with displacement of 0.5mm.

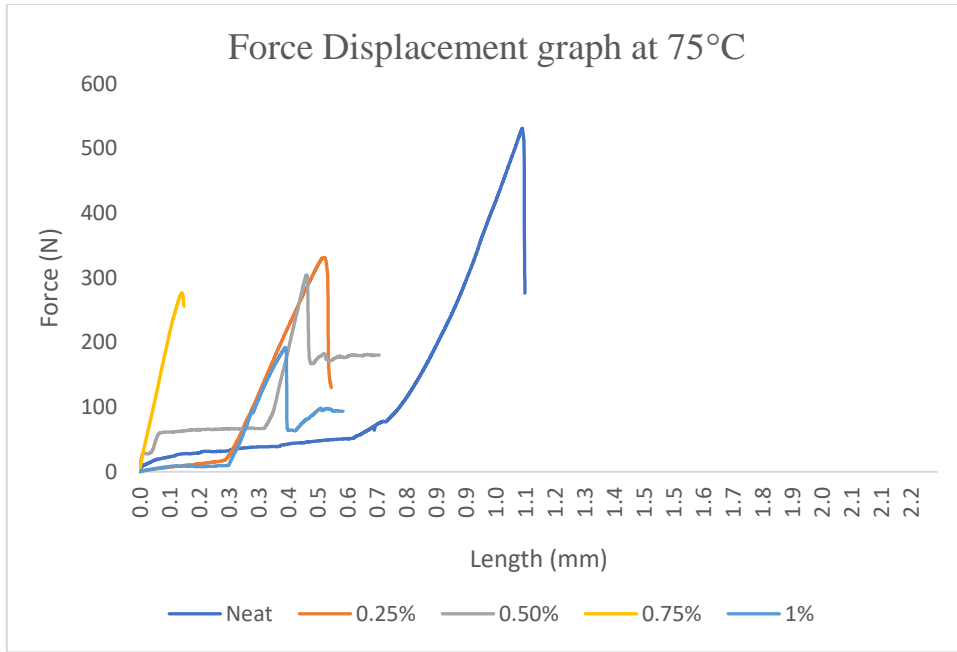
From the study of all graphs for different concentrations and different temperature, it can be concluded that as the concentration of cork increased the value of failure load decreases, it has also been seen that with the increases in temperature the failure load also decreases due to change in the properties of adhesive. Overall, the effect of increases in concentration and temperature is negative to strength of the joint. The joint shows that neat solution adhesive joint has more strength against all temperatures when compared with the joint of cork concentration.



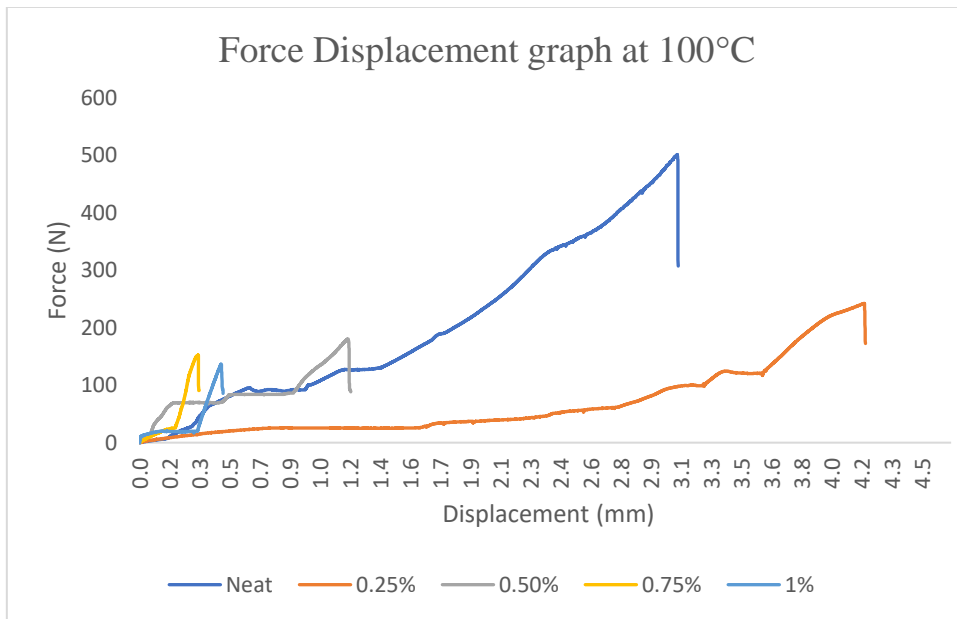
**Figure 4.10:** Force displacement curve at 25°C temperature and at different concentration



**Figure 4.11:** Force displacement curve at 50°C temperature and at different concentration



**Figure 4.12:** Force displacement curve at 75°C temperature and at different concentration



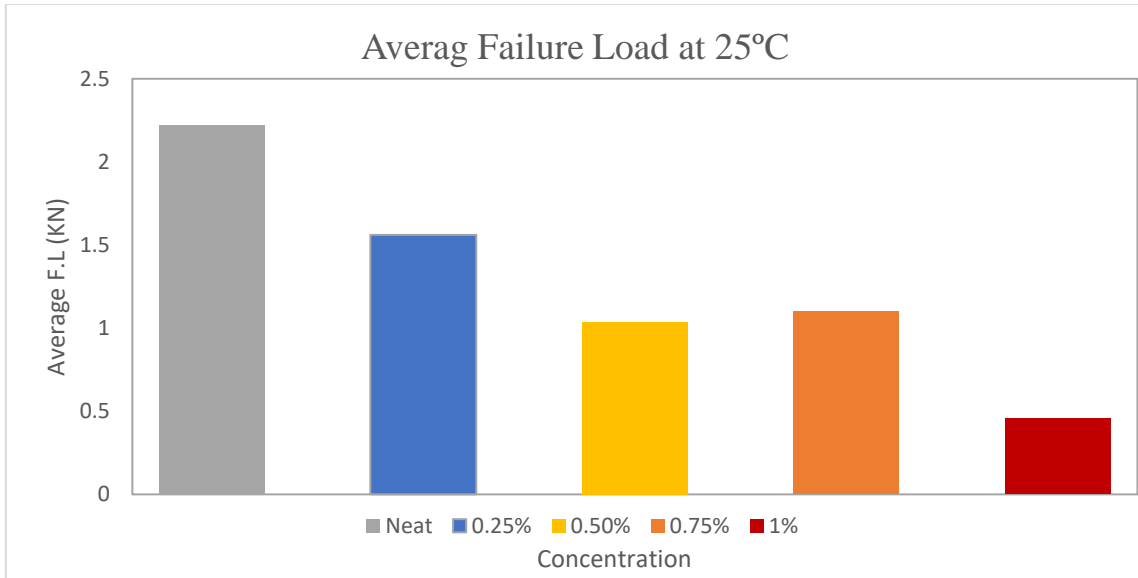
**Figure 4.13:** Force displacement curve at 100°C temperature and at different concentration

Fig. 4.14 shows the average failure load for different concentrations and at 25 degrees temperature. Graph shows the highest failure load for neat adhesive with value of 2.22KN. Failure load decreased from neat adhesive to 0.5 wt.%. Lowest failure load recorded for 1 wt.% with value of 0.456KN. Failure load for 0.25 wt.% was recorded for 1.56KN. 1.037KN average failure load was recorded for 0.5 wt.%. Average failure load for 0.75 wt.% increased as compared to 0.50 wt.% and recorded value was 1.1KN.

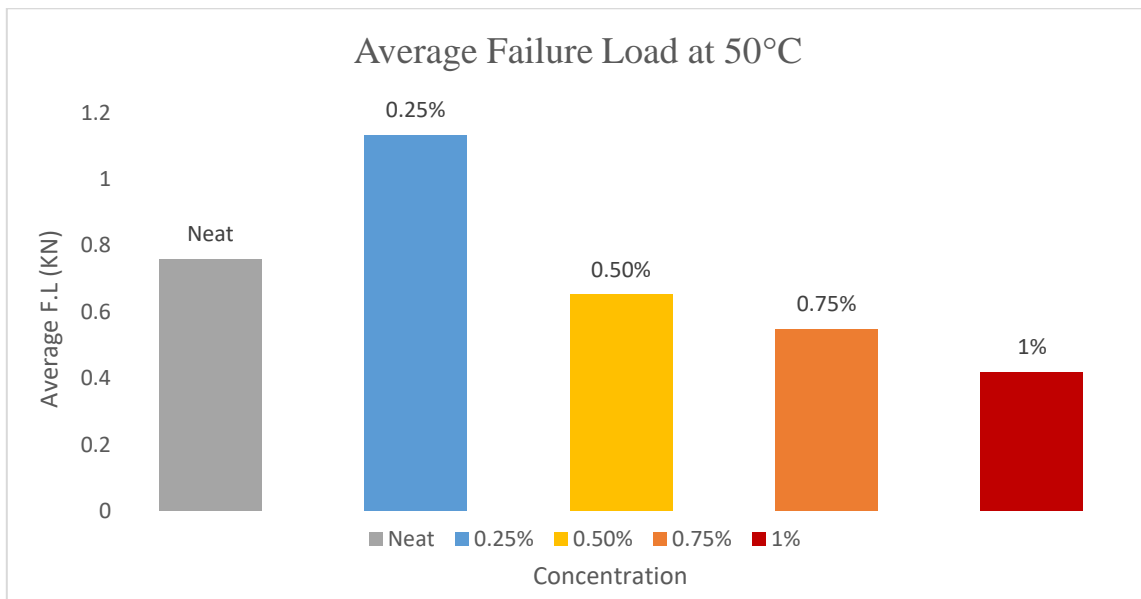
Fig. 4.15 illustrated the average failure load for different concentrations and at 50 degrees temperature. The result shows the highest average failure load for 0.25 wt.% with value of 1.13KN. The lowest average failure load recorded for 1 wt.% with value of 0.147KN. The average failure load was 0.575KN for neat adhesive. 0.651KN was recorded average failure load for 0.5 wt.%. The average failure load recorded for 0.75 wt.% with value of 0.546KN. It was also seen that failure loads decreases from 0.25 wt.% to 1 wt.%.

Fig 4.15 shows the average failure load from 0.25 wt.% to 1 wt.% at 75 degrees temperature. The highest average failure load recorded for 0.75 wt.% with value of 0.496KN. the lowest average failure load recorded for 1 wt.% with value of 0.192KN. It was seen from the graph that average failure load increases from 0.25 wt.% to 0.75 wt.% and then decreases for 1 wt.%. Average failure load recorded for 0.25 wt.% was 0.251KN. 0.386KN average failure load recorded for 0.5 wt.%. The average failure load recorded for neat solution was 0.382KN.

Fig 4.16 shows the average failure load at different concentrations and at 100 degrees temperature. Average failure load decrease from neat solution to 0.5 wt.% and then increased for 0.75 wt.%. The highest average failure load recorded for neat adhesive with value of 0.302KN. The average failure load for 0.25 wt.% recorded with value of 0.261KN. The average failure load for 0.5 wt.% was 0.13KN. 0.167KN average failure load recorded for 0.75 wt.%. The lowest average failure load recorded for 1 wt.% with value of 0.09KN. So, it can be concluded that overall effect of cork concentration on joint is negatives.



**Figure 4.14:** Average failure load of tubular joint at 25°C and at different cork concentrations



**Figure 4.15:** Average failure load of tubular joint at 50°C and at different cork concentrations

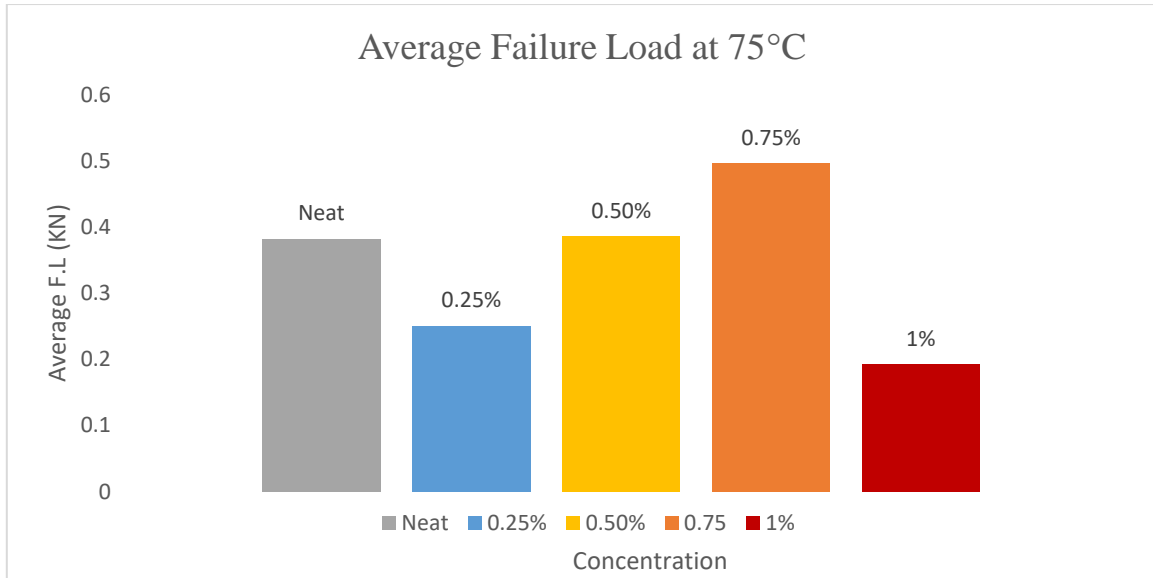


**Figure 4.16:** Average failure load of tubular joint at 75°C and at different cork concentrations

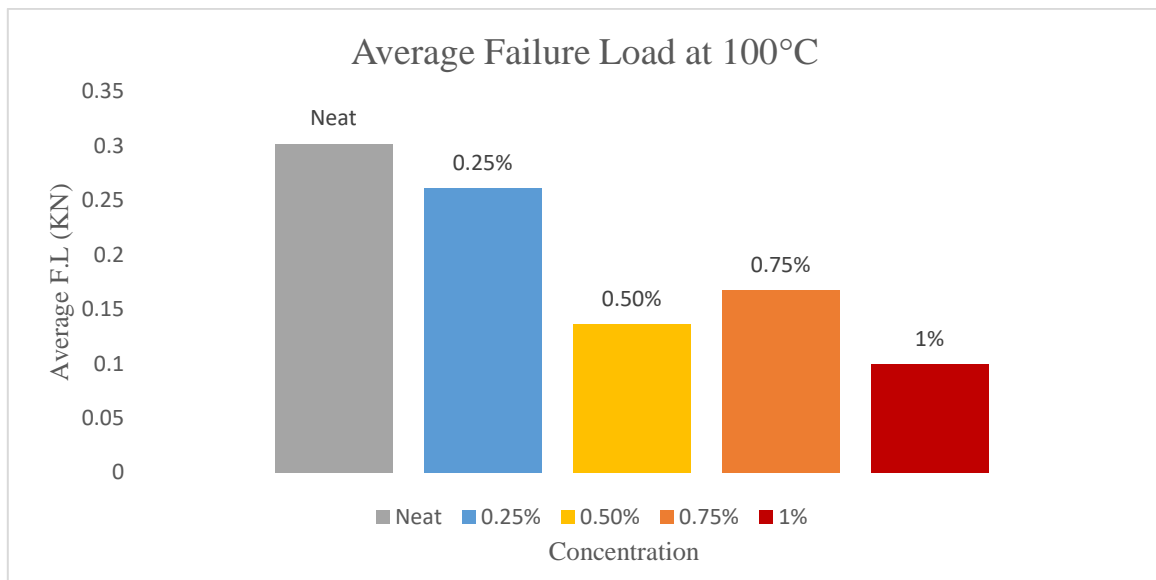


**Figure 4.17:** Average failure load of tubular joint at 100°C and at different cork concentrations

**Table 4-4:** Average failure load at different concentrations and at different temperatures

| Serial No. | Concentration | Average F.L at 25°C in KN | Average F.L at 50°C in KN | Average F.L at 75°C in KN | Average F.L at 100°C in KN |
|------------|---------------|---------------------------|---------------------------|---------------------------|----------------------------|
| 1          | Neat          | 2.22                      | 0.75                      | 0.38                      | 0.30                       |
| 2          | 0.25 wt.%     | 1.56                      | 1.13                      | 0.25                      | 0.26                       |
| 3          | 0.50 wt.%     | 1.04                      | 0.65                      | 0.38                      | 0.136                      |
| 4          | 0.75 wt.%     | 1.10                      | 0.54                      | 0.496                     | 0.167                      |
| 5          | 1 wt.%        | 0.46                      | 0.42                      | 0.192                     | 0.099                      |

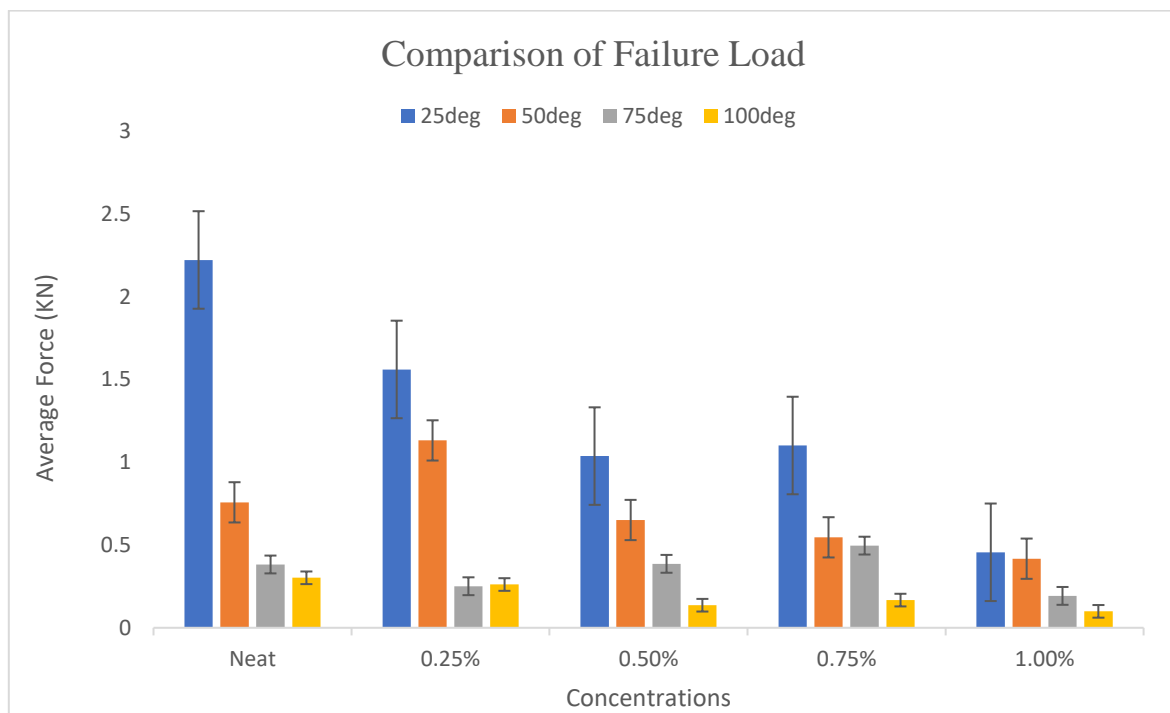


**Figure 4.18:** Comparison of average failure load at different temperatures and at different concentrations.

**Table 4-5:** Failure load comparison at different temperatures and at different concentrations with reference to room temperature.

| <b>Concentration</b> | <b>Temperature</b> | <b>Effect (%)</b> |
|----------------------|--------------------|-------------------|
| Neat                 | 25°C               |                   |
|                      | 50°C               | -65.8964          |
|                      | 75°C               | -82.7906          |
|                      | 100°C              | -86.4066          |
| 0.25 wt.%            | 25°C               |                   |
|                      | 50°C               | -                 |
|                      | 75°C               | 27.4727           |
|                      | 100°C              | -                 |
| 0.50 wt.%            | 25°C               |                   |
|                      | 50°C               | -                 |
|                      | 75°C               | 37.2227           |
|                      | 100°C              | -                 |
| 0.75 wt.%            | 25°C               |                   |
|                      | 50°C               | -                 |
|                      | 75°C               | 62.7450           |
|                      | 100°C              | -                 |
| 1 wt.%               | 25°C               |                   |
|                      | 50°C               | -8.4795           |
|                      | 75°C               | -57.7485          |
|                      | 100°C              | -78.2163          |



**Table 4-6:** Failure load comparison of neat with different cork concentrations at different temperatures

| <b>Temperature</b> | <b>Concentration (wt.%)</b> | <b>Effect (%)</b> |
|--------------------|-----------------------------|-------------------|
| 25°C               | 0                           |                   |
|                    | 0.25                        | -29.7674          |
|                    | 0.50                        | -53.323333        |
|                    | 0.75                        | -50.442610        |
|                    | 1                           | -79.474868        |
| 50°C               | 0                           |                   |
|                    | 0.25                        | -49.362076        |
|                    | 0.50                        | -14.07831         |
|                    | 0.75                        | -27.89265         |
|                    | 1                           | -44.918609        |
| 75°C               | 0                           |                   |
|                    | 0.25                        | -34.350479        |
|                    | 0.50                        | 1.046207          |
|                    | 0.75                        | 29.816913         |
|                    | 1                           | -49.607672        |
| 100°C              | 0                           |                   |
|                    | 0.25                        | -13.465783        |
|                    | 0.50                        | -54.856512        |
|                    | 0.75                        | -44.591611        |
|                    | 1                           | -67.108167        |

## Chapter 5: Conclusion

Analysis of tubular adhesive joints carried out to determine the strength of two different material joints with galvanised steel pipe. In first layout CPVC socket used as outer material and steel pipe as inner material. In second layout PVC socket used as outer material and galvanised steel pipe to make joint with epoxy adhesive Araldite-LY-556 and hardener AD-22962. Tests were performed at four different temperatures 25°C, 50°C, 75°C and 100°C and concentrations include neat adhesive joints and cork concentrations includes 0.25 wt.% to 1 wt.% for both layouts of joints.

- (i). Adhesive behaviour was brittle to make higher strength of joints so that it can replace the welded and bolts joints. Although epoxy shows higher strength against small displacements. Cork powder was added to decrease the crack propagation against strength which was not the case of neat adhesive.
- (ii). In case of CPVC and steel joints, from failure load-displacement graph it can be concluded that strength start decreases from 0.25 wt.% to 1 wt.% at 25°C temperature with highest value was achieved at 0.25 wt.% cork concentration. But in case of PVC and steel pipe layout, it can be concluded that with increase in cork concentration the strength of the joint decreases. The highest failure load was achieved for neat adhesive joint and lowest for 1 wt.% cork concentration at 25°C temperature.
- (iii). At 50°C for CPVC it is concluded that failure load increases from neat solution to 0.25 wt.% and then decreases for 0.50 wt.% and increase for 0.75 wt.% and finally decreases for 1 wt.%. In case of PVC and steel pipe joint, it is concluded that with increase in cork concentrations the failure load decreases. Largest displacement against failure load recorded for 0.25 wt.%.
- (iv). At 75°C for CPVC, highest failure load recorded for 0.75 wt.%. Failure load decreases from neat adhesive to 0.25 wt.% while increases from 0.50 wt.% to 0.75 wt.%. the lowest failure load recorded for 1 wt.%. In case of PVC and steel pipe layout failure load decreases from neat adhesive to 1 wt.% in which highest failure load achieved for neat adhesive while lowest at 1 wt.% cork concentration.
- (v). At 100°C in case of CPVC the highest failure load achieved for 0.75 wt.% cork concentration and lowest for 1 wt.%. Failure load increases from neat adhesive to 0.75 wt.% and decreases for 1 wt.%. In case of PVC and steel tubular layout, it has been concluded that failure load decreases from neat adhesive to 1 wt.% cork concentration.

- (vi). It can be concluded from average failure load for CPVC and steel pipe that highest failure load recorded for 0.25 wt.% at 50°C and lowest average failure load recorded for 1 wt.% at 100°C. For neat adhesive highest failure load recorded for 25°C and lowest for 100°C. For 0.25 wt.% adhesive highest failure load recorded at 50°C and lowest for 100°C. for 0.50 wt.% highest failure load recorded at 50°C and lowest at 100°C. At 0.75 wt.% the highest failure load recorded at 25°C and lowest at 100°C. For 1 wt.% the highest failure load recorded at 25°C, and lowest failure load recorded at 100°C. Overall spectrum of failure loads decreased from 0.25 wt.% to 1 wt.%.
- (vii). For PVC and steel tubular joints, results of average failure loads shows that average failure loads were highest at 25°C and lowest at 100°C for neat adhesive and from 0.25 wt.% to 1 wt.% cork concentration. It has also been concluded that with increase in temperature failure loads decreased. Overall spectrum of results shows that neat adhesive has highest average failure load while lowest for 1 wt.% cork concentration.

## References

- [1] M. A. C. R. J. C. M. E. A. S. K. D. & D. S. L. F. M. Dantas, “Flexible tubular metal-polymer adhesive joints under torsion loading,” *International Journal of Adhesion and Adhesives*, pp. 105, 102787., 2021.
- [2] F. Marchione, “Simplified static shear strength prediction model for adhesively bonded joints assembled with brittle adhesives,” *Mechanics Research Communications*, pp. 127, 104022, 2023.
- [3] M. M. F. A. O. P. R. K. & R. B. C. Hiremath, “Investigation of adhesively bonded multi-material joints: An assessment on joint efficiency and fracture morphology,” *Materials Today: Proceedings*, pp. 27, 1180-1185, 2020.
- [4] E. & G. L. Dragoni, “Adhesive stresses in axially-loaded tubular bonded joints–Part I: Critical review and finite element assessment of published models.,” *International Journal of Adhesion and Adhesives*, vol. 47, pp. 35-45, 2013.
- [5] A. E. S. C. R. D. S. G. M. R. D. F. & S.-A. I. J. Pinheiro, “Validation of theoretical models for the strength prediction of tubular adhesive joints,” *Procedia Structural Integrity*, pp. 41, 60-71, 2022.
- [6] A. & M. P. Parashar, “Adhesively bonded composite tubular joints,” *International Journal of Adhesion and Adhesives*, vol. 38, pp. 58-68, 2012.
- [7] M. F. M. O. C. R. D. S. G. & M. R. D. F. Rosas, “Numerical analysis of geometrical modification combinations of the tensile strength of tubular adhesive joints,” *Procedia Structural Integrity*, pp. 33, 115-125, 2021.
- [8] S. & D. J. M. Labbé, “ A multi-objective optimization procedure for bonded tubular-lap joints subjected to axial loading,” *International journal of adhesion and adhesives*, vol. 33, pp. 26-35, 2012.
- [9] M. A. C. R. J. C. M. E. A. S. K. D. & D. S. L. F. M. Dantas, “Flexible tubular metal-polymer adhesive joints under torsion loading,” *International Journal of Adhesion and Adhesives*, pp. 105, 102787, 2021.
- [10] I. Z. C. & T. K. T. Kaiser, “Mechanical behavior and failure mechanisms of CFRP and Titanium tubular adhesive lap joints at extreme temperatures,” *Composite Structures*, pp. 290, 115528, 2022.
- [11] F. F. M. & G. P. Heidarpour, “Experimental investigation of the effects of adhesive defects on the single lap joint strength,” *International journal of adhesion and adhesives*, vol. 80, pp. 128-132, 2018.

- [12] D. K. W. P. H. K. A. S. M. R. S. S. K. A. .. & G. N. K. Rajak, “Impact of fiber reinforced polymer composites on structural joints of tubular sections: A review,” *Thin-Walled Structures*, pp. 180, 109967, 2022.
- [13] M. V. T. F. H. & U. T. Albiez, “Adhesively bonded steel tubes—Part I: Experimental investigations,” *International Journal of Adhesion and Adhesives*, pp. 90, 199-210, 2019.
- [14] S. & J. M. Aimmanee, “Stress analysis of adhesive-bonded tubular-coupler joints with optimum-stiffness-composite adherend under axial tension, pressure, and thermal loading,” *International Journal of Adhesion and Adhesives*, p. 103343, 2023.
- [15] J. E. S. M. C. R. D. S. G. S.-A. I. J. & M. R. D. F. Silva, “Numerical evaluation of tensile-loaded tubular scarf adhesive joints,” *Procedia Structural Integrity*, pp. 41, 36-47, 2022.
- [16] A. E. S. C. R. D. S. G. M. R. D. F. & S.-A. I. J. Pinheiro, “Validation of theoretical models for the strength prediction of tubular adhesive joints,” *Procedia Structural Integrity*, pp. 41, 60-71, 2022.
- [17] T. M. E. M. K. M. Y. B. & G. X. Higgoda, “Experimental investigation on the structural behaviour of novel non-metallic pultruded circular tubular GFRP T-joints under axial compression,” *Thin-Walled Structures*, pp. 184, 11051, 2023.
- [18] H. C. M. A. P. G. W. Y. & C. M. S. Biscaia, “Influence of uniform temperature variations on hybrid bonded joints with a circular or tubular cross-sectional area,” *Mechanics of Materials*, pp. 179, 104600, 2023.
- [19] T. J. S. C. R. D. S. G. C. M. G. & S.-A. I. J. Oliveira, “Cohesive zone analysis of torsional tubular joints with an epoxy adhesive,” *Procedia Structural Integrity*, pp. 41, 72-81, 2022.
- [20] A. W. M. A. & M. M. Rudawska, “Effect of ageing process on mechanical properties of adhesive tubular butt joints in aqueous environment,” *International Journal of Adhesion and Adhesives*, pp. 96, 102466, 2020.
- [21] N. P. B. O. K. Z. D. & B. R. Lavalette, “Influence of geometrical parameters on the strength of Hybrid CFRP-aluminium tubular adhesive joints,” *Composite Structures*, pp. 240, 112077, 2020.
- [22] I. & T. K. T. Kaiser, “Damage and strength analysis of Carbon Fiber Reinforced Polymer and Titanium tubular-lap joint using hybrid adhesive design,” *International Journal of Adhesion and Adhesives*, pp. 103, 102710, 2020.
- [23] J. A.-S. A. C. R. J. C. M. E. A. S. G. R. & d. S. L. F. M. Antelo, “Fatigue life evaluation of adhesive joints in a real structural component,” *International Journal of Fatigue*, pp. 153, 106504, 2021.

- [24] M. V. Çakır, “The synergistic effect of hybrid nano-silica and GNP additives on the flexural strength and toughening mechanisms of adhesively bonded joints,” *International Journal of Adhesion and Adhesives*, pp. 122, 103333, 2023.
- [25] J. A.-S. A. C. R. J. C. M. E. A. S. G. R. & d. S. L. F. M. Antelo, “Replacing welding with adhesive bonding: An industrial case study,” *International Journal of Adhesion and Adhesives*, pp. 113, 103064, 2022.
- [26] A. H. & C. D. S. Ibrahim, “Mechanical testing of adhesive, self-piercing rivet, and hybrid jointed aluminum under tension loading,” *International Journal of Adhesion and Adhesives*, pp. 113, 103066, 2022.
- [27] L. R. F. C. R. D. S. G. B. D. R. R. J. B. & S. F. J. G. Ferreira, “Static strength improvement of tubular aluminium adhesive joints by the outer chamfering technique,” *Procedia Manufacturing*, vol. 38, pp. 629-636, 2019.
- [28] S. Z. R. K. A. B. & Z. M. Braiek, “Experimental and numerical study of adhesively bonded±55 filament wound tubular specimens under uniaxial tensile loading,” *Composite Structures*, vol. 172, pp. 297-310, 2017.
- [29] J. K. O. H. D. S. M. J. F. A. N. C. & H. C. Kosmann, “Measurement of epoxy film adhesive properties in torsion and tension using tubular butt joints,” *International Journal of Adhesion and Adhesives*, vol. 83, pp. 50-58, 2019.
- [30] R. R. B. N. V. K. & C. A. Das, “Fluid-structure interaction based adhesion failure analysis of bonded tubular socket joints., 144, .,” *Procedia Engineering*, vol. 144, pp. 1260-1269, 2016.
- [31] Z. B. Y. H. X. J. L. & Z. L. Zhang, “Cyclic performance of bonded sleeve beam-column connections for FRP tubular sections,” *Composites Part B: Engineering*, vol. 142, pp. 171-182, 2018.
- [32] J. L. H. Y. L. H. & J. H. Zhang, “Investigation on fatigue performance of adhesively bonded butt-joints and multiaxial life estimation using stress-based failure models. , 107, .,” *Theoretical and Applied Fracture Mechanics*, vol. 107, p. 102498, 2020.
- [33] A. & D. E. Spaggiari, “Regularization of torsional stresses in tubular lap bonded joints by means of functionally graded adhesives,” *International Journal of Adhesion and Adhesives*, vol. 53, pp. 23-28, 2014.
- [34] G. V. D. U. H. V. H. B. & D. S. Fernandez, “Experimental identification of static and dynamic strength of epoxy based adhesives in high thickness joints,” *International Journal of Solids and Structures*, vol. 120, pp. 292-303, 2017.
- [35] J. B. T. L. É. S. G. D. S. D. & T. D. Le Pavic, “Failure load prediction of a tubular bonded structures using a coupled criterion,” *Theoretical and Applied Fracture Mechanics*, vol. 108, p. 102531, 2020.

- [36] R. R. & B. N. Das, “Failure analysis of bonded composite pipe joints subjected to internal pressure and axial loading,” *Procedia Engineering*, vol. 144, pp. 1047-1054, 2016.
- [37] S. & K. M. A. Kumar, “An elastic solution for adhesive stresses in multi-material cylindrical joints,” *International Journal of Adhesion and Adhesives*, vol. 64, pp. 142-152, 2016.
- [38] M. M.-P. A. A. F. & L. F. Lamberti, “Influence of web/flange reinforcement on the GFRP bonded beams mechanical response: A comparison with experimental results and a numerical prediction,” *Composite Structures*, pp. 147, 247-259., 2016.
- [39] M. H. F. S. C. T. H. T. G. J. C. & B. J. B. Kabir, “ Experimental and numerical investigation of the behaviour of CFRP strengthened CHS beams subjected to bending.,” *Engineering Structures*, pp. 113, 160-173, 2016.
- [40] M. H. F. S. C. T. H. T. & B. M. Kabir, “Durability of CFRP strengthened steel circular hollow section member exposed to sea water,” *Construction and Building Materials*, pp. 118, 216-225., 2016.
- [41] X. B. Y. L. F. J. Z. X. L. & D. F. Yang, “Dynamic and fatigue performances of a large-scale space frame assembled using pultruded GFRP composites.,” *Composite Structures*, pp. 138, 227-236., 2016.
- [42] K. P. B. M. A. F. S. M. K. V. G. .. & d. M. À. Triantou, “Performance of cork and ceramic matrix composite joints for re-entry thermal protection structures,” *Composites Part B: Engineering*, pp. 108, 270-278, 2017.
- [43] S. M. J. A. M. R. E. E. & D. S. L. F. M. Razavi, “Mixed-mode fracture response of metallic fiber-reinforced epoxy adhesive.,” *European Journal of Mechanics-A/Solids*, pp. 65, 349-359, 2017.
- [44] A. Q. D. S. L. F. M. A. J. F. M. & Ö. A. Barbosa, “Toughness of a brittle epoxy resin reinforced with micro cork particles: Effect of size, amount and surface treatment,” *Composites Part B: Engineering*, pp. 114, 299-310, 2017.
- [45] M. V. T. & U. T. Albiez, “Adhesively bonded steel tubes–Part II: Numerical modelling and strength prediction,” *International Journal of Adhesion and Adhesives*, pp. 90, 211-224, 2019.
- [46] S. M. L. & C. R. D. S. G. Eusebio, “Modelling of tubular adhesively-bonded joints by the Extended Finite Element Method,” *Procedia Manufacturing*, pp. 41, 484-491, 2019.
- [47] B. W. T. E. & H. P. Hahn, “Experimental and numerical investigations on adhesively bonded tubular connections for moulded wooden tubes,” *Construction and Building Materials*, pp. 229, 116829, 2019.

- [48] V. & S. K. S. Darla, "Evaluation of strength and performance for a single lap bonded joint by insertion of structural elements in adhesive," *International Journal of Adhesion and Adhesives*, vol. 118, p. 103240, 2022.
- [49] K. & K. Y. Gültekin, "The effect of boron nanoparticle reinforcement on the structural and mechanical performance of nanocomposites and bonded joints exposed to an acid environment.," *International Journal of Adhesion and Adhesives*, vol. 118, p. 1032, 2022.
- [50] Y. & G. K. Korkmaz, "Improvement of structural, thermal and mechanical properties of epoxy composites and bonded joints exposed to water environment by incorporating boron nanoparticles," *International Journal of Adhesion and Adhesives*, vol. 116, p. 103141, 2022.
- [51] S. Kumar, " Analysis of tubular adhesive joints with a functionally modulus graded bondline subjected to axial loads," *International Journal of Adhesion and Adhesives*, vol. 29(8), pp. 785-795, 2009.
- [52] J. H. Oh, "Nonlinear analysis of adhesively bonded tubular single-lap joints for composites in torsion," *Composites science and technology*, Vols. 67(7-8), pp. 1320-1329, 2007.
- [53] A. & D. E. Spaggiari, "Regularization of torsional stresses in tubular lap bonded joints by means of functionally graded adhesives," *International Journal of Adhesion and Adhesives*, vol. 53, pp. 23-28, 2014.